Contributions to the Chemistry of Boron, 210[1]

η^2-Transition Metal Complexes of the Ligand 9-Fluorenylidene(2,2,6,6-tetramethylpiperidino)borane

Scott W. Helm[a], Gerald Linti[a], Heinrich Nöth*[a], Sreelatha Channareddy[a], and Peter Hofmann*[b]

Institut für Anorganische Chemie der Universität München[a],
Meiserstraße 1, W-8000 München 2, F.R.G.

Laboratorium für Anorganische Chemie der Technischen Universität München[b],
Lichtenbergstraße 4, W-8046 Garching, F.R.G.

Received August 12, 1991

Key Words: 9-Fluorenylidene(tetramethylpiperidino)borane ligand / Iron complexes / Cyclopentadienyl ligands / Calculations, MO

The boraolefin 9-fluorenylidene(tetramethylpiperidino)borane **L** forms complexes **1**–**4** with the isolobal fragments $Fe(CO)_4$, $CpCo(CO)$, $Cp'Mn(CO)_2$, and $C_6H_6Cr(CO)_2$, respectively. Compounds $FeL(CO)_3PR_3$ (PR_3 = PMe_3, $PhPMe_2$, Ph_2PMe, PCl_3, $PhPCl_2$, **1 a**–**e**) are obtained photochemically from $Fe(CO)_5$, **L**, and PR_3 in toluene solution. An X-ray structure analysis **1** and **1 a** reveals a distorted trigonal-bipyramidal geometry, with the boron atom of **1** in an equatorial position. **2** contains two independent molecules in the asymmetric unit. The two molecules are enantiomers with Co atoms in a pseudotetrahedral environment. MO calculations demonstrate that the distortion found in **1** is due to electronic rather than steric effects as exemplified by the model compound $Fe(CO)_4(H_2N{-}B{=}CH_2)$ (**6**). π-Back bonding from the metal-centred 2a′ orbital to the boron-centred π^*_{BC} orbital contributes significantly to the stablilization of the energy-minimized structure **8**. Experimental evidence for this back bonding is provided by the shorter M–B bond in **1** and **2** as compared with the M–C bond to the boraoelfin unit. However, the reverse is true for the manganese complex **3**.

The chemistry of compounds containing boron groups connected to transition metal centres has expanded rapidly during the past two decades[2]. Many of the complexes involve acid-base interactions[3] or bonding through a hydride bridge[4]. Transition metal boryl complexes which are expected to contain metal–boron σ-bonds[5] have only recently been characterized by X-ray diffraction methods[6]. However, a much larger body of structural information is available for metallaboranes and metallacarboranes[7]. Considerable interest focusses also on the chemistry of boron heterocycles formed by the formal replacement of sp^2 carbon in the organic π centres by sp^2-boron atoms and their interaction with metal-containing fragments[8]. These boron heterocycles act as strong electron acceptors towards transition metal moieties giving access to mononuclear complexes analogous to metallocenes and metal-arene π complexes. Many X-ray structural studies[9] demonstrate that, although boron in these compounds is within the bonding distance of the metal, the metal atom tends to slip away from the boron atoms towards the more electronegative ring atoms, and thus the differences between the bond lengths d(M–B) and d(M–C) are usually larger than differences between the respective covalent radii of boron and carbon alone.

Presently, there is considerable interest in the synthesis of boron-carbon[10] and boron-nitrogen[11] multiple bond systems. Though several transition metal complexes of (alkylimino)- and amino-imino-boranes are known[12], some of them bind the metal fragments by the imino nitrogen lone pair [12d]. On the other hand, (9-fluorenylidene)(2,2,6,6-tetramethylpiperidino)borane (**L**), the first kinetically stabilized amino-alkylidene-borane[10b], possesses a much less polar B=C bond and is consequently found to behave more like an asymmetrically substituted olefin. Thus, amino-alkylidene-boranes typically undergo [2 + 2] and [2 + 3] cycloaddition reactions involving the B=C double bond[13]. Moreover, **L** can coordinate to transition metal fragments, as demonstrated for the complex $Fe(CO)_4(\eta^2\text{-}L)$ (**1**)[14]. We report here on an extension of these studies including a MO description of the bonding in $(CO)_4Fe(\eta^2\text{-}H_2C{=}B{-}NH_2)$ as a model for $(CO)_4Fe(\eta^2\text{-}L)$.

Results and Discussion

Complex **1**[14] can be isolated in 48% yield from the reaction of **L** with $Fe_2(CO)_9$ in toluene under ambient conditions. The same complex is obtained in higher yield (64%) by photolysis of $Fe(CO)_5$ using a slight deficiency of the ligand **L**. The formation of complex **1** by this method is depicted in Scheme 1.

Although the photolysis method has found wide use in the synthesis of olefin iron carbonyl complexes, disadvantages of this method have been noted[15] which are due to the possible loss of two equivalents of CO to yield a mixture of the mono and diolefin species. In the present situation,

  0009–2940/92/0101–0073 $ 3.50+.25/0

Scheme 1

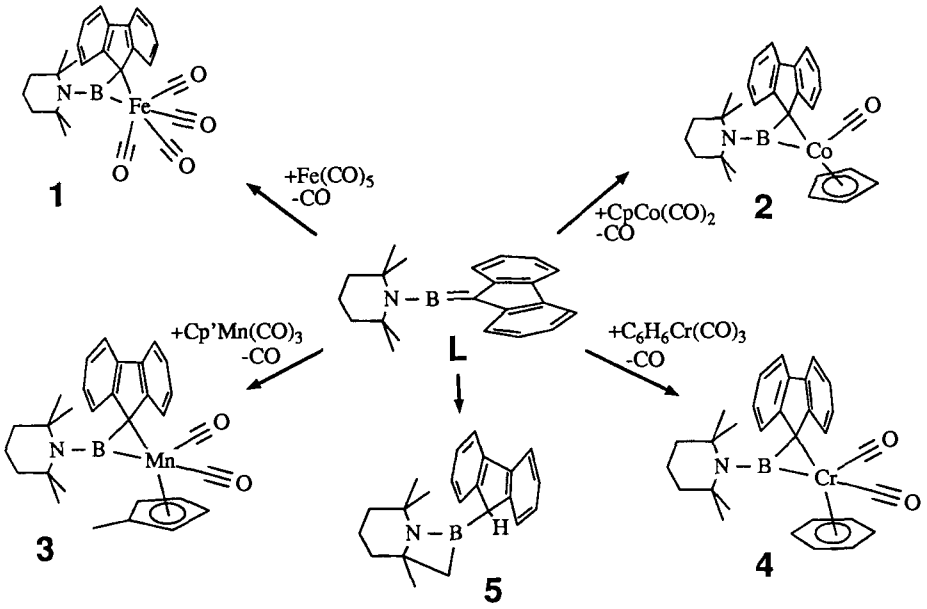

the formation of the single product **1** can reasonably be explained on the basis of two aspects,
i) the ligand is sterically demanding and the formation of $Fe(CO)_3(\eta^2\text{-}\mathbf{L})_2$ therefore unlikely, and
ii) the complex $Fe(CO)_3(\eta^4\text{-}\mathbf{L})$[16] is obtained only on prolonged irradiation of **L** and $Fe(CO)_5$.

Attempts to synthesize complex **2** from $CpCo(CO)_2$ and **L** under ambient conditions or in refluxing toluene have been unseccessful. The photolysis of $CpCo(CO)_2$, however, in the presence of an equimolar amount of the ligand **L** leads to the formation of $CpCo(CO)(\eta^2\text{-}\mathbf{L})$ (**2**), which crystallizes from toluene/hexane as dark red-brown prisms.

Irradiation of $(Cp')Mn(CO)_3$ (Cp′ = methylcyclopentadienyl) in the presence of an equimolar amount of **L** affords complex **3** as a yellow microcrystalline solid. It is essential for its preparation that the reaction mixture is flushed with nitrogen gas before stopping the irradiation since the ligand **L** can be readily replaced by CO, thus reversing the reaction. Similary, the photolysis of a solution containing $(C_6H_6)Cr(CO)_3$ and **L** results in the formation of the orange-colored complex **4** which is isolated in 69% yield.

Attempts to replace the olefin ligands in $(Ph_3P)_2Pt(C_2H_4)$ and $Ni(COD)_2$ (COD = cyclooctadiene) by **L** have failed. Both complexes induce a rearrangement of the ligand **L** to the product **5** as shown in Scheme 1. Although the mechanism of this catalytic reaction is not known, product **5** has thoroughly been characterized by spectroscopic methods[17].

Spectroscopic Data

The ^{11}B-NMR spectra of the complexes **1**–**4** show one signal in the region δ = 57.2–61.2 which represents no significant change from the starting material **L**[10b], although the peak width has substantially decreased by 300–350 Hz. Inspection of ^{11}B-NMR data reveals a slight downfield shift as one moves from Cr to Co. This observation implies that the electronegativity of the metal bound to boron seems to be responsible for the changes in shielding within this series of compounds.

The 2,2,6,6-tetramethylpiperidino (tmp) ring protons in ligand **L** have resonances between δ^1H = 1.51 and 1.77, but these extend over a much larger range in the complexes **1**–**4**. Furthermore, two sharp singlets, each integrating to six protons, are found for the methyl groups in **1**–**4** whereas only one singlet for the four methyl groups is observed in **L**. Whether more than one signal arises from these methyl protons cannot be exactly determined for complex **2** due to signal broadening from paramagnetic impurities. However, the large splitting for the Cp ring protons (at least five different signals can be identified, lying at intervals of 0.2 ppm) implies both hindered rotation about the B–N bond as well as a loss of symmetry compared with complex **1**. This has been expected since the cobalt compound has no centre of symmetry being bound to the Cp group on one side and to CO and L in the other side.

In the ^{1}H-NMR spectrum of **3** four Cp protons split into two groups of 2 H atoms. Though this inequivalence can be explained by the symmetry of the Cp′ ring provoked by the presence of the methyl group, the magnitude of this difference ($\Delta\delta$ = 0.27 ppm) is large when one considers that these CH protons are found to be equivalent in the starting material $Cp'Mn(CO_3)$[18]. The reason for this splitting has later been recognized from the crystal structure determination (see Figure 2) where two of the four protons are directly situated above the fluorenyl ring and are subject to an anisotropic highfield shift whereas the remaining two are located farther away from the fluorene ring system and are therefore observed in the expected region. Similar to **3** we have found in the ^{1}H-NMR spectrum of **4** that the protons of the arene ligand attached to the Cr atom are divided into two sets of three protons each at δ^1H = 3.31 and 3.99 in-

dicating the lack of a symmetry plane perpendicular to the fluorene ring.

The ^{13}C-NMR spectrum of **1** shows seven signals in the aliphatic region for tmp carbon atoms. They are, furthermore, all shifted to a relatively low filed implying a significant loss of electron density most likely through a strong BN-(pp)-π interaction. Another interesting feature is the presence of only six signals for the twelve carbon atoms of the fluorenyl unit. This indicates that the molecule possesses a plane of symmetry. The signals are found at an extremely low field relative to the uncoordinated ligand. The atoms C10 and C10′[19] particulary are considerably shifted downfield by 9.3 and 4.7 ppm, respectively. A similar pattern is also observed for the aliphatic region of the complexes **3** and **4**, but for complex **2** a total of nine ^{13}C-NMR signals are found for the tetramethylpiperidino carbon atoms. This is due to the inequivalence of the methyl groups bound to the carbon atoms C2 and C6. One of the methyl groups is situated *cis* to the Cp ring and the other *cis* to the CO group resulting in the non-equivalence of all tmp-methyl groups. Although the fluorenyl region of **3** is similar to **1**, compound **2** shows twelve signals which are found for the two six-membered rings confirming the lack of symmetry. In compound **1** the symmetry with respect to the fluorene moiety is, however, not as perfect as might be expected. This is demonstrated by the presence of the four signals attributed to C10, C10′, C15, and C15′.

In the manganese compound **3** the signal for the methyl Cp's group is observed at $\delta^{13}C = 101.9$. Signals for the other carbon atoms of the Cp ring are consistent with its ^{1}H-NMR spectrum. Two resonances are found at $\delta^{13}C = 89.8$ and 90.9 which are significantly deshielded as compared to the starting material ($\delta^{13}C = 82.3$)[18] proving an unsymmetrical environment for the Cp group. Similarly, and in accord with the ^{1}H-NMR spectrum, the ^{13}C-NMR spectrum of **4** shows three different signals at $\delta = 97.8$, 100.0, and 104.3 for the π-bonded benzene ring implying the presence of a plane of symmetry which passes through the middle of two opposite C–C bonds of the benzene ring.

At room temperature only one ^{13}C-NMR signal is found for the carbonyl carbons in **1**–**3** and two signals in compound **4**. However, the low-temperature spectrum of **1** (231 K) reveals three signals in a 1:1:2 ratio at $\delta = 209.4$, 207.8, and 206.6. This proves a fluxional behaviour of the CO groups, particularly for **1** at ambient temperature. At low temperature a static structure is achieved, and both number and intensity of the CO signals indicate a trigonal-bipyramidal environment with two CO groups in the apical and two in the equatorial plane.

The ^{13}C-NMR signal for the boron- and metal-bound C9 carbon atoms is observed in the range of $\delta = 21.7-27.8$ for compounds **1**–**4**, close to the position for olefinic carbon atoms bound directly to the first-row transition metals[20], e. g. this signal is shifted from the sp^2 state for C9 in **L** to the sp^3-hybridized range on complexation.

The IR spectrum of **1** exhibits three ν(CO) bands at 2064, 2011, and 1962 cm^{-1}. A shoulder is attached to the 1962 cm^{-1} band at 1971 cm^{-1} consistent with the ^{13}C-NMR observation that there are altogether three nonequivalent CO groups in **1**. Similary, the IR spectra of **2**–**4** show the expected number of CO streching vibrations ranging from 1841 to 1958 cm^{-1}, respectively. In contrast to the starting materials $CpCo(CO)_2$, $Cp'Mn(CO)_3$, and $C_6H_6Cr(CO)_3$, all these bands are found at lower frequency indicating a poorer π-acceptor quality for the ligand tmp-B=CR_2 relative to the CO group. The final spectroscopic proof that the B= C unit is coordinated η^2-wise to the metal carbonyl units comes from the IR spectra as well: The absorption at 1717 cm^{-1} attributed to ν(N=B=C) in the uncoordinated ligand **L**[10b,f] has disappeared in the compounds **1**–**4**.

Molecular Structures of 1–3 in the Solid State

In order to ascertain the structures of **1**–**4** and to get information on the configuration, the conformation, and on other structural details an X-ray study has been made. Selected bonding parameters are summarized in Table 1.

Table 1. Selected bond distances and bond angles in compounds **1**–**4**. Estimated standard deviations are quoted in parentheses

Bond Distances in Å		M-B	M-C	B-C	B-N	M-P
1[10f]	(M=Fe)	2.125(5)	2.190(4)	1.518(7)	1.377(6)	
2	(M=Co)	2.011(8)	2.073(6)	1.513(8)	1.376(8)	
		1.989(10)	2.075(6)	1.495(9)	1.407(8)	
3	(M=Mn)	2.162(5)	2.148(4)	1.518(5)	1.396(5)	
1a	(M=Fe)	2.091(4)	2.159(4)	1.521(5)	1.393(4)	2.229(2)
1f[16]	(M=Fe)	2.116(10)	2.175(9)	1.535(12)	1.364(11)	2.181(3)
Bond angles in °						
		B-M-C	M-C-B	C-B-M	M-B-N	C-B-N
1		41.2(2)	67.1(2)	71.7(2)	146.0(3)	142.3(4)
2		41.2(2)	67.1(2)	71.7(2)	146.0(3)	142.3(4)
		43.5(2)	66.1(4)	70.5(4)	146.0(5)	143.6(7)
3		41.2(1	69.9(2)	68.9(2)	151.1(3)	140.0(4)
1a		41.9(1)	66.7(2)	71.3(2)	147.7(3)	140.7(3)
1f		41.9(3)	67.0(5)	71.1(5)	146.3(7)	142.5(9)

An ORTEP plot of **1** has already been depicted[14], and a different view is included in Figure 3. The coordination around the iron atom can be regarded in the first place as distorted trigonal-bipyramidal. The equatorial plane is defined by the iron atom, mid point of the boraolefin bond and two carbonyl carbon atoms while the other two carbonyl groups occupy the apical positions. Although it seems conceivable that the bulky ligand **L** forces the bond angle between the axial carbonyls to become much smaller [151.2(2)°] than the 180° found in $Fe(CO)_5$, MO calculations (discussed later in this paper) suggest that the observed distortion is not an outcome of steric effects but of electronic origin. The B–C bond length in **1** has increased by 0.1 Å relative to the free ligand **L** [1.420(3) Å][10f] similar to the lengthening of a C=C bond on π complexation, a well established fact for metal olefin complexes[21] due to synergic effects. Consequently, the N–B–C1 bond angle deviates

from linearity as shown by the bond angle of 142.3(4)° in contrast to 177.7(2)° in **L**[10f]. The B–N bond length of 1.377(6) Å indicates a significant double bond character[11a], as has already been deduced from the ^{1}H- and ^{13}C-NMR spectra. The C21–N–C25 plane of the tetramethylpiperidine ring lies almost parallel to the Fe-B-C1 plane with an angle between the normals to these planes of only 4.7°.

The midpoint of the B=C unit of **1** is situated in the equatorial position with the B=C double bond lying approximately in the equatorial plane. This mode of coordination for an olefin is found in almost all pentacoordinate d^8 transition metal-olefin complexes and has been predicted by Hoffmann et al.[22] and Veillard et al.[23] for olefins and other single faced π acceptors. The sensible reason for such an arrangement is that it provides for optimum π-back bonding interactions.

It has been stressed[14] that the observed Fe–B bond length [2.125(5) Å] is shorter than the Fe–C bond [2.190(4) Å] inspite of the larger covalent radius of the boron atom. Therefore, boron plays a dominant role as π acceptor. This is in agreement with Florianis finding[24] that the stability of $Fe(CO)_4(\eta^2$-heterocumulene) complexes is largely determined by the π interaction between the C=X fragment (in our case B=C) and the d orbitals of the metal atom. This fact is corroborated by the MO calculations described later. Furthermore, viewing the boron atom as the stronger Lewis acid centre, the Fe–B bond would be expected to be shorter due to stronger back donation from the metal orbitals. This is also demonstrated for the Fe–C bond lengths in $Fe(CO)_4(C_2H_4)$ (2.12 Å)[25] and $Fe(CO)_4(C_2F_4)$ (1.99 Å)[26].

Since the boraolefin occupies an equatorial position, it is the equatorial metal-carbonyl distances that should be most affected. In general, olefinic ligands are weaker π acids than CO groups, and it is the equatorial carbonyl that is more tightly bound to the iron centre as shown for $Fe(CO)_4L$ complexes (L = η^2-acenaphthylene[21], η^2-[3-methylene-*exo*-4-vinyl-dihydrofuran-2(3*H*)-one[27], η^2-*cis*-bis(methoxycarbonyl)methylenecyclopropane[27b], and $L[Fe(CO)_4]_2$[28]). Only with the very strong π acceptors $CF_2=CF_2$ does the reverse appear to be true[26]. In complex **1**, the Fe–C_{eq} bonds lengths [1.820(5) Å] are longer than the Fe–C_{ax} lengths of 1.786(5) Å, indicating a π acidity of the boraolefin comparable to $CF_2=CF_2$.

Compound **2** crystallizes with 1 molecule of toluene per 2 molecules of **2**. A stick and ball model is depicted in Figure 1 a, and an ORTEP plot of one of the two independent molecules of **2** in Figure 1 b. The molecules formally contain tetrahedrally coordinated Co atoms (considering the centre of the Cp ring as a point atom) carrying four different substituents. Therefore, **2** must be optically active. Consequently, the two independent molecules in Figure 1 a are enantiomers. As described above for **1**, the most noticeable change in the geometry of the ligand **L** is the lack of its allenic type structure and the lengthening of the B=C bond. The latter corresponds well with the B–C1 bond length found in **1** [1.513(8) and 1.518(5) Å, respectively]. Again, the Co–B bond lengths [2.000(8) Å average] are shorter than the Co–C distance [2.074(6) Å average] underlining the

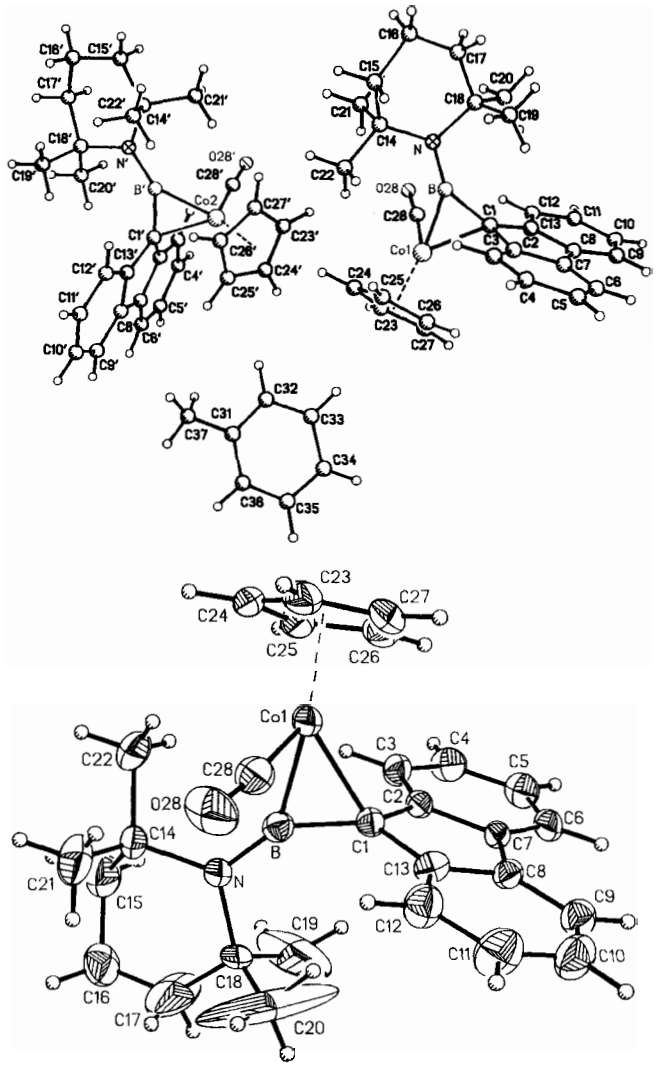

Figure 1. a) The two independent molecules of **2** and the toluene molecule of the asymmetric unit. b) ORTEP plot of one of the two molecules of complex **2**. Thermal ellipsoids are shown at the 30% probability level

conclusion drawn from the structure of **1**. The B–N–C1 atoms are bent by an bond angle of 143.6(7)°, and the B–N bond length is as short as in **1**. The C14–N–C18 plane of the tetramethylpiperidino group is slightly twisted out from the Co1–B–C1 plane as shown by an interplanar angle of 14.9°. However, the Co atom, the CO group, and the midpoint of the B=C unit form a perfect plane while the B=C unit is not perpendicular to this plane but is tilted by an angle of 19.7°. This twist is, therefore, stronger than in **1**.

The Co–(CO) bond length [1.696(6), 1.714(7) Å] is shorter and the C–O bond distance [1.167(8), 1.157(8) Å] is longer as compared to 1.728(8) and 1.136 Å in $(\eta^5$-$C_5Me_5)Co(CO)_2$[29], respectively. This can be rationalized as follows: since only one CO group is present in complex **2**, stronger back bonding to the B=C unit should increase the C=O double bond character for the carbonyl group. The C–C and Co–C distances and bond angles for the cyclopentadienyl ligand correspond with those found in a number of related **structures**[29].

Figure 2 shows the crystal structure of complex **3** demonstrating the same general structural features as found for **1** and **2**. However, whereas the metal-carbon distances to L in **1** and **2** have been found to be longer than the metal-boron distances by 0.065 and 0.062 Å, respectively, the Mn – B bond is now 0.014 Å *longer* than the Mn – C1 bond. While a mean value for $d(M-BC) = (d_{M-B} + d_{M-C})/2 =$ 2.16(1) Å results for **1** and **3** this average distance is only 2.04 Å in **2**. It seems, therefore, that the metal-boron and metal-carbon bond lengths change with the number of CO groups present at a metal centre. The B – N bond length [1.393(5) Å] in **3** is longer than that found in **1** and **2**, but its double bond character nonetheless remains uneffected.

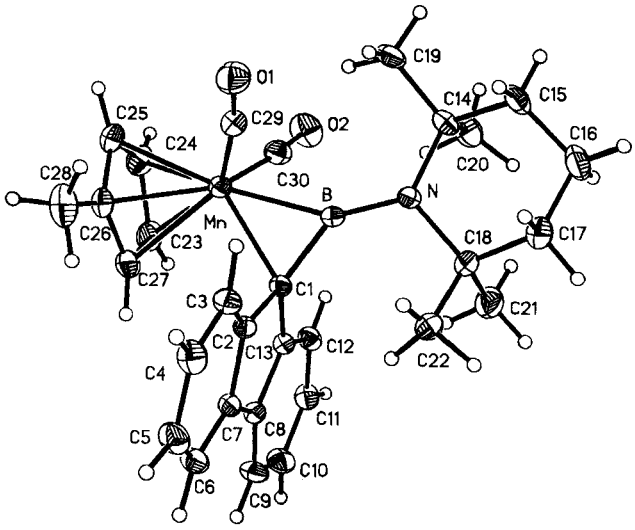

Figure 2. ORTEP plot of a molecule **3** in the crystal. Thermal ellipsoides are drawn on the 30% probability level

The angle C1 – Mn – B [41.2(1)°] is identical to the corresponding angle at the Fe atom in **1** and somewhat more acute than the angle C1 – Co – B [43.5(2)°] in **2**. Consequently, the angle Mn – B – C1 at boron, 68.9°, is slightly smaller than the corresponding angles Fe – B – C1 [71.7(2)°] and Co – B – C1 [70.5(4)°].

The average Mn – C distance to the methylcyclopentadienyl group results as 1.767 Å. This is shorter than the corresponding value for $CpMn(CO)_3$ [1.797(20) Å][30], $CpMn(C_7H_8)(CO)_2$ [1.794(7) Å][31], and $CpMn(CH_2 = CHCOCH_3)(CO)_2$ [1.787(7) Å][32]. Also the average C – O distance, 1.165 Å, is longer in **3** than those found in the above cited structures. The same explanation as given for the short Co – CO distance can also be applied here.

The geometry at the Mn centre of **3** is pseudo-tetrahedral as evidenced by an angle of 103.4(2)° formed between the two carbonyl groups at the Mn atom. The corresponding angles are 91.9(4)° for $CpMn((C_7H_8)(CO)_2$ and 88.8(4)° for $CpMn(CH_2 = CHOCMe)(CO)_2$. The carbonyl groups in **3** are somewhat bent, the deviations from linearity being 8.3 and 9.3°, respectively.

MO Calculations

In order to obtain more insight into the electronic structure and bonding situation in the boraolefin complexes, molecular orbital calculations of extended Hückel type[33] have been performed for a simplified model of complex **1**, namely $(CO)_4Fe(H_2N-B=CH_2)$ (**6**) (see Figure 3). Because of the more "flexible" tetracarbonyliron fragments, **6** should reflect best how the metal subunit responds to the electronic requirements of the methylene borane ligand as its bonding partner. The observed overall molecular geometry of **1** can be quantiatively described in two different ways, viewing the B = C ligand either in an equatorial or in an axial position of a rather severely distorted trigonal bipyramid, a rather well understood phenomenon for $(CO)_4Fe(C_2H_4)$[25]. The following discussion is based on the geometry of **1** and its

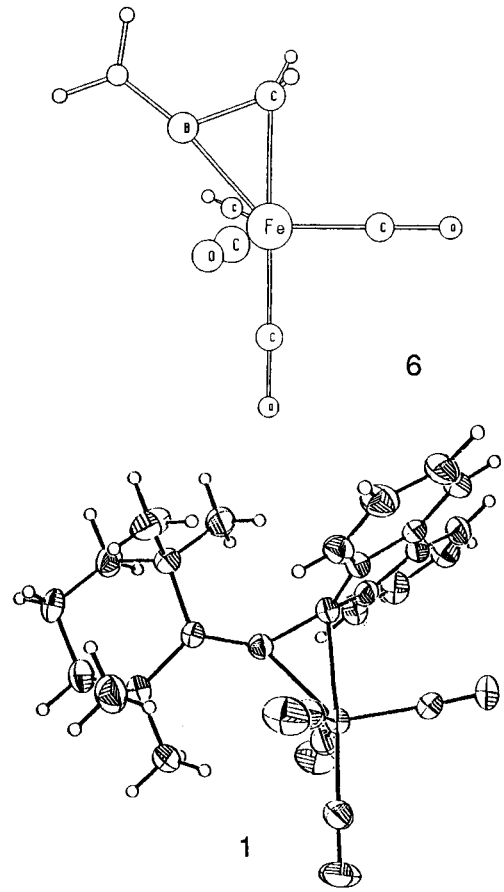

Figure 3. Structure of the model compound $(CO)_4Fe(H_2N-B=CH_2)$ (**6**) as compared to the molecular structure of **1** in the solid state

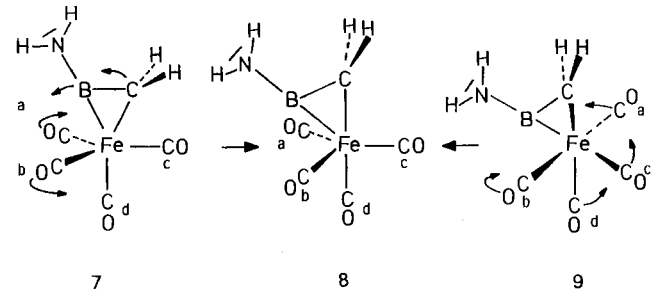

Figure 4. Respresentation of the distortion of two limiting cases: trigonal-bipyramidal [$C_{3v}Fe(CO)_4$ fragment] **7** and distored-bipyramidal [$C_sFe(CO)_4$ fragment] **9** arrangement towards the best fit **8**

model **6** as being derived from an "idealized" trigonal bipyramid with the η^2-methyleneborane ligand bound symmetrically in an axial position as shown in **7** by opening up the equatorial $CO_a-Fe-CO_b$ angle to approximately 150° and by bending over the complete $H_2N-B=CH_2$ unit towards an opening angle (arrow in **7**) until the methyleneborane carbon, iron atom, and the axial CO group of **7** are colinear (C_s symmetry preserved throughout) as shown in Figure 4.

The ground-state situation **8** (actual geometry plotted in **6**) obtained by this method is practically identical to the observed geometry of **1**. It can be alternatively portrayed as being derived from **9**, an undistorted trigonal-bipyramidal geometry with equatorial $H_2N-B=CH_2$ in which two axial carbonyl groups ($CO_{a,b}$) bend towards each other in the boron direction and the two equatorial CO ligands ($CO_{c,d}$) move as indicated by arrows in Figure 4 until configuration **8** is reached. Obviously, either description is equally valid, and the final geometry **8** is somewhere in between **7** and **9**[34].

The starting point for the MO calculations is the "undistorted" model **7**. The first question to be answered is whether the observed geometry of **1** is the result of the rather large substituents at the B=C unit since it seems conceivable that the widened C_a-Fe-C_b angle in **1** (151.2° as compared to 120° in **6**) is caused by the tetramethylpiperidino group[10]. In **7** steric crowding would be minimized. However, even for the uncongested model the energy minimum is found for the geometry plotted in **6** which results when both the equatorial C_a-Fe-C_b angle and the angle between the *trans*-C_b and the $Fe-CH_2$ bond of **7** are optimized independently. These angles optimize at values of 140 and 179°, respectively. Starting from **9** and optimizing the angles C_a-Fe-C_b, $C_c-Fe-CH_2$, and C_d-Fe-C_c gives **8** as well. Therefore, the specific coordination geometry of **1** must be of electronic rather than steric origin which may well be augmented by steric effects in **1** where the methyl group-substituted piperidine ring instead of the simple in-plane NH_2 group of **7** approaches two equatorial CO groups and squeezes them further apart than in the model complex. The relaxation from **7** to **8** stabilizes the molecule by not more than 4.6 kcal/mol, and by even less, if we start from **9**. The small energy differences between ideal and relaxed structure is of course consistent with the well-known tiny energy barriers for Berry-type pseudorotations of d^8-ML_5 compounds, e. g. $Fe(CO)_5$ or of $Fe(CO)_4(C_2H_4)$[35].

The four molecular orbitals of an amino-substituted methyleneborane ligand $H_2N-B=CH_2$ are similar to those

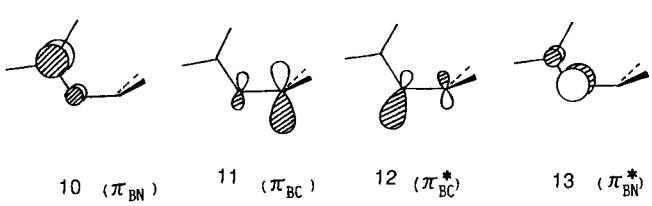

Figure 5. Representation of the BC-π orbitals. Energy increases in the order **10** to **13**

of an η^2-bound allene, e. g. in $(CO)_4Fe(H_2C=C=CH_2)$ as schematically depicted in Figure 5.

Their MO energies ascend from **10** to **13** as shown in Figure 5, in accord with simple electronegativity and perturbation considerations[36]. The two frontier levels are **11** (HOMO, π_{BC}) and **12** (LUMO, π^*_{BC}), separated by approximately 2 eV from **10** (π_{BN}) and **13** (π^*_{BN}), respectively. These frontier MOs **10** and **11** are shown as contour diagrams within the H_2NBC plane in Figure 6.

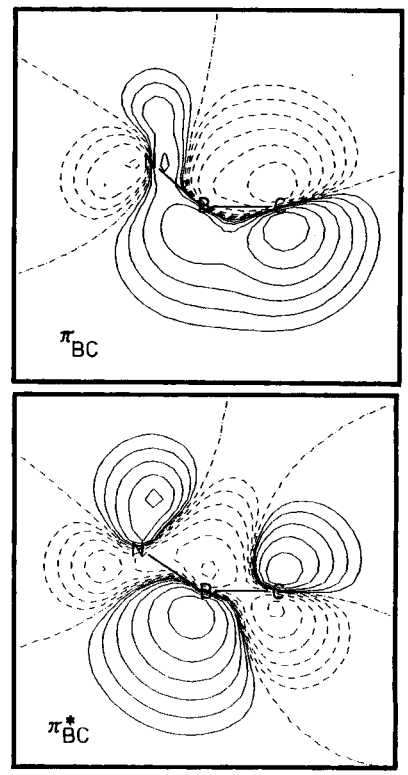

Figure 6. Contour plots for $H_2N-B=CH_2$ frontier MOs **11** and **12** in the NBC plane. The contours represent values of 0, +/−0,0125, +/−0.025, +/−0.05, +/−0.1, +/−0.2, +/−0.4 of the wave functions

As expected from basic perturbation theory arguments[36], the coefficients at the boron and carbon atom of the B=C unit are very different in both the π_{BC} orbital and in its antibonding counterpart π^*_{BC}. In our calculations π_{BC} is localized with 87% at carbon ("C lone pair"), while π^*_{BC} carries 80% of its wave function on the boron atom. In both MOs the usual rehybridization occurs, which at boron is due to the bent N−B−C skeleton, and at carbon to some pyramidalization[37], which improve ligand-to-metal overlap[38].

In order to analyze the electronic structure of $(CO)_4Fe(H_2N-B=CH_2)$, we begin with the undistorted geometry of **7**. Figure 7 shows an interaction diagram for this model with the methyleneborane unit bound symmetrically in an axial position. At the left hand side are the valence levels of a $Fe(CO)_4$ fragment with C_{3v} symmetry[39], and at the right hand side are the orbitals of the ligand $H_2N-B=CH_2$. Of these, only π_{BC} and π^*_{BC} interact strongly with $Fe(CO)_4$ va-

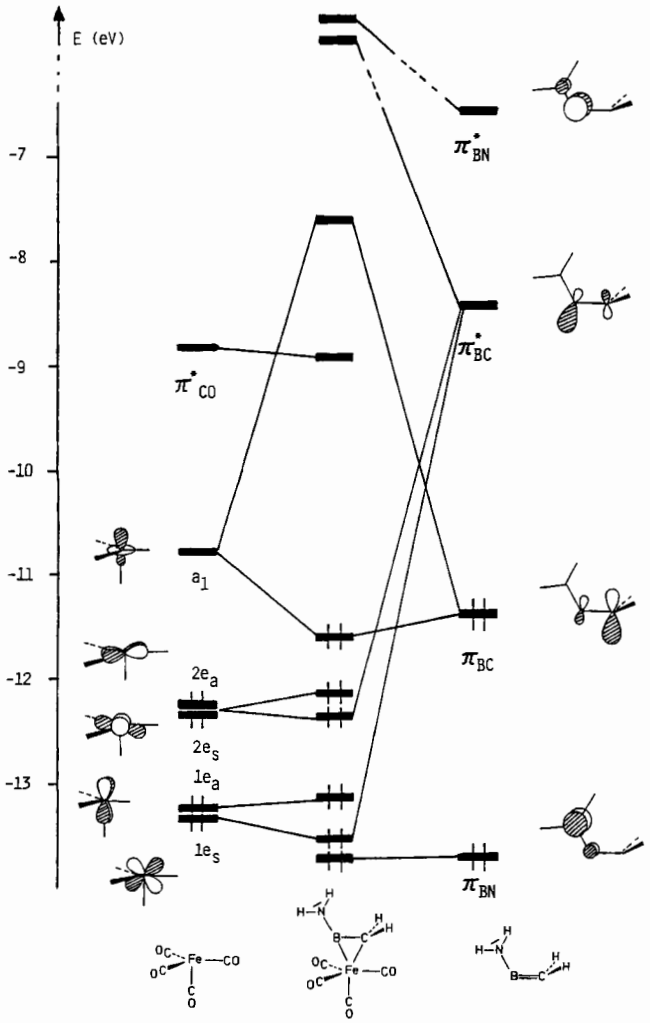

Figure 7. Orbital interactions diagram between an $Fe(CO)_4$ fragment (C_{3v}) and a $H_2N-B=CH_2$ ligand for the undistorted geometry of **7**. Only the metal contribution to the $Fe(CO)_4$ orbitals and one of the low-lying π^*CO levels are shown for simplicity

lence levels. The ligand HOMO overlaps with the LUMO (a_1, mainly z^2) of the metal fragment, their bonding combination forms the HOMO of the complex with 69% ligand character. This interaction represents most of the ligand-to-metal donation, transferring 0.591 electrons from π_{BC} to $Fe(CO)_4$. The acceptor level of the tetracarbonyliron moiety receives a total of 0.788 electrons from the amino-methyleneborane ligand. The low-lying π^*_{BC}-MO interacts with the two symmetric components of the two filled $Fe(CO)_4$ e-sets. $1e_s(xz)$ is slightly more stabilized by this ligand-to-metal back donation than $2e_s(x^2 - y^2)$ for overlap reasons, although the latter is the donor level which is closer in energy to π_{BC}. Both metal orbitals lose approximately the same amount of charge to the ligand ($1e_s$: 0.150 e, $2e_s$: 0.165 e). The total charge transfer from $Fe(CO)_4$ to the LUMO π_{BC} amounts to 0.936 e for the undistorted trigonal-bipyramidal geometry **7**. The overall Mulliken charge of the $H_2N-B=CH_2$ fragment in the molecule is +0.333, i.e. back bonding returns only half of the electron density that is lost by the dative π_{BC}-orbital-to-$Fe(CO)_4$ interaction for an unrelaxed structure **7**.

This situation is drastically changed by going from **7** to **8** (= **6**), and we can analyze this energetically favourable distortion in two steps by:

i) describing the consequences of changing the $Fe(CO)_4$ fragment geometry from C_{3v} (in **7**) to C_2 (in **8**) as described by Figure 8,

ii) by analyzing the changes for $Fe(CO)_4-H_2N-B=CH_2$ bonding when reaching the minimum energy structure **8** (see Figure 9).

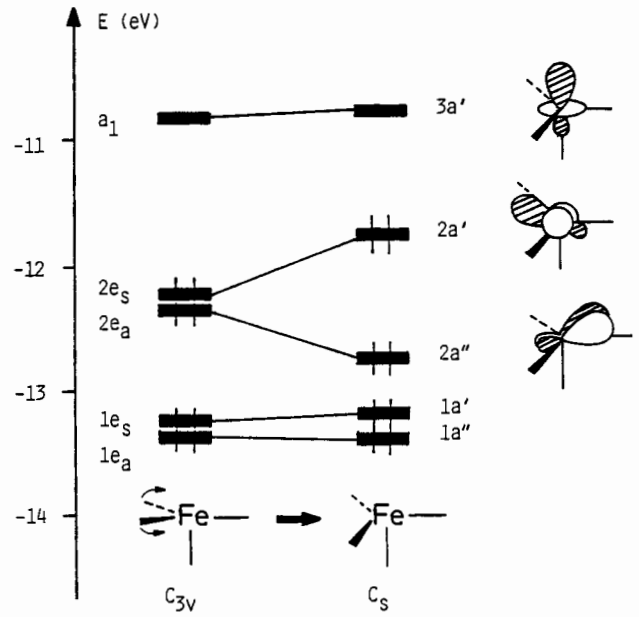

Figure 8. Orbital energy changes for the distortion of the $Fe(CO)_4$ fragment from C_{3v} (as in **7**) to C_s (as in **9** or **1**)

While the orbitals 1e and $1a_1$ remain practically unaffected, it is the 2e set (mainly $x^2 - y^2$ and xy at Fe) which exhibits a pronounced splitting in energy. The symmetric level $2e_s$ ($x^2 - y^2$) is destabilized due to reduced overlap and back bonding with the π^* levels of the two moving CO ligands, which simultaneously interact more strongly in a destabilizing σ antibonding fashion with the metal centre. Exactly the opposite is the case for the $2e_a(xy)$ orbital which is pushed to lower energy compared to the C_{3v} structure, where both the ($x^2 - y^2$) and (xy) orbitals experience by symmetry identical π-back bonding and σ repulsion. It is obvious that such a C_{3v}-to-C_2 fragment distortion, abandoning some back bonding to two equatorial carbonyl groups, is improving the $Fe(CO)_4$ fragment's capability to function as a metal π donor towards a fifth ligand of appropriate symmetry and of porper location in the empty axial position[40]. As seen from Figure 7, level 2a' of the fragment $Fe(CO)_4$ in C_2 symmetry is not only a higher energy than the $2e_s$ orbital had been in the undistorted C_{3v} metal fragment, but its still dominant ($x^2 - y^2$) character also suggests that the optimal back bonding to an axial ligand should be only possible for in-plane π acceptor orbitals located off-axis. Given the previously discussed appearance of the MO **12**, the LUMO π^*_{BC} of an $H_2N-B=CH_2$ ligand, it

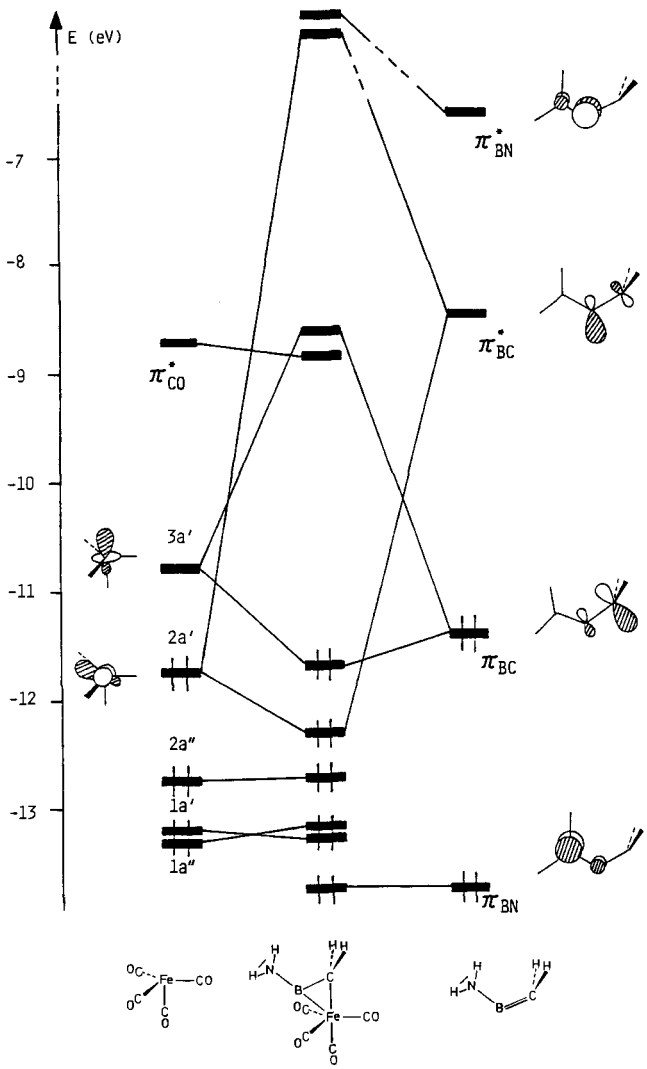

Figure 9. Orbital interaction diagram between a distorted $Fe(CO)_4$ fragment (C_s) and the $H_2N-B=CH_2$ ligand for the geometry of **8**. Only the metal contributions to the $Fe(CO)_4$ orbitals and the lowest lying of the π^*CO orbitals are shown for simplicity

becomes immediately clear, why **8** is found as the minimum energy structure. Figure 9 represents the relevant interaction scheme, constructing **8** now from the distorted $Fe(CO)_4$ fragment and the properly positioned methyleneborane ligand.

Back bonding now occurs exlusively from $2a'(x^2 - y^2)$ to π^*_{BC}, i.e. from the highest occupied d level of $Fe(CO)_4$ to the LUMO of the ligand. The three lower-filled metal orbitals are not involved but remain available for back bonding to the CO groups. In the distorted geometry **8** the large lobe of π^*_{BC} (at boron) overlaps with the large lobe of 2a', and similarly the large lobe of π_{BC} (at carbon) overlaps with the large lobe of the metal fragment's σ acceptor MO 3a' in the z axis, while the repulsive interaction of π_{BC} with $1a'(xy)$ of $Fe(CO)_4$ is minimal. So, in the specific geometry of **8** (and **1**) both Fe–B and Fe–C bonding are optimized, and in particular back bonding is improved. This is reflected in the Mulliken charge of the $H_2N-B=CH_2$ fragment in **8**: it drops from +0.333 in **7** to +0.096, i.e. both the ligand and the iron fragment are essentially neutral. The π^*_{BC} acceptor level receives 0.469 electrons in **8**, the 2a' metal donor orbital loses 0.350 electrons to the ligand. The Fe–C overlap population increases from 0.165 in **7** to 0.255 for **8**, the Fe–B overlap population remains practically unchanged (0.25). Table 2 lists computed overlap integrals between valence MOs of the $Fe(CO)_4$ fragment and the $H_2N-B = CH_2$ ligand for both molecular geometries **7** and **8** (= **6**).

Table 2. Fragment MO overlap integrals between $H_2N-B=CH_2$ and $Fe(CO)_4$ valence orbitals for geometries **7** and **8**, respectively

	Overlaps		
6	$<\pi^*_{BC}/2e_s> = 0.1861$	$<\pi^*_{BC}/1e_s> = 0.1551$	$<\pi_{BC}/a_1> = 0.1981$
7 (= **5**)	$<\pi^*_{BC}/2a'> = 0.2632$	$<\pi^*_{BC}/1a'> = 0.0948$	$<\pi_{BC}/3a'> = 0.1950$

Back donation from the iron orbital HOMO 2a' to the methyleneborane ligand LUMO π^*_{BC} is improved by geometric relaxation. The specific structures of $(CO)_4Fe(H_2N-B=CH_2)$ and of **1** create an electronic situation, where an ethylene-like π system with pronounced asymmetry (i.e. having formally one donor and one acceptor end of the double bond) can be bound to the $Fe(CO)_4$ unit in such a way as to place the donor terminus (here the C atom) into the axial position of the resulting trigonal bipyramid, while good back bonding to the acceptor end is retained at a "quasi" equatorial site. This is in accordance with the known ligand site preference rules for d^8 trigonal-bipyramidal complexes[22a]. The atomic Mulliken charges in **8** indicate an appreciable electron deficiency at boron (charge: +0.878) and a negative charge accumulation at carbon of the $H_2N-B=CH_2$ ligand (charge: −0.648), which are certainly overestimated by the EHMO model used here. They do, however, represent the correct trend of charge distribution, and obviously the tetramethylpiperidino group at boron and the aromatic π system, into which the coordinated carbon is incorporated in compound **1**, are ideal to delocalize charge density and to exert an overall stabilizing effect.

We also note, that the manifold of lowest unoccupied orbitals for $(CO)_4Fe(H_2N-B=CH_2)$ is of π^*_{CO} character, localized predominantly in the CO ligand (only the one at lowest energy is included in Figures 7 and 9). Radical anion chemistry or photochemistry may accordingly be governed by CO loss[16] and would be of interest, as well as the oxidation chemistry of **1** and of its relatives. The experimental observation of just one ^{13}C-NMR signal for the CO groups in **1** is in line with the small energy differences for all possible conformers along a pseudorotation rearrangement pathway.

Compared to other metal fragments as coordinating groups for aminomethyleneboranes [e.g. $CpMn(CO)_2$, CpCo(CO) etc.] the $Fe(CO)_4$ moiety is geometrically more flexible in adapting to the electronic demands of the methyleneborane-ML_n system, and this may be the reason, why the stronger back bonding to the boron end has its clearest reflection in an even shorter B–Fe than C–Fe bond in **1**.

Reactions of 1 with Phosphanes and Other Ligands

Direct substitution of CO groups in complex **1** by other π-acidic ligands is found to be difficult. Phosphanes do not react with **1** under ambient and thermal conditions. However, irradiation of complex **1** in the presence of an equimolar amount of a phosphane leads to the displacement of $tmp-B=CR_2$ to give a mixture of $Fe(CO)_4(PR_3)$ and $Fe(CO)_3(PR_3)_2$[41]. A similar situation is found when a mixture of equimolar amounts of the ligand, $Fe(CO)_5$, and PR_3 is subjected to photolysis. But it has been observed that the addition of phosphanes to a solution of **1** in toluene, which is irradiated by a mercury lamp until eventually one equivalent of CO is liberated, affords the expected phosphane-substituted derivatives **1 a–e** in 63–71% yield as shown in Scheme 2. These compounds are quite stable and reluctant to further substitution.

Reaction of **1** with four equivalents of *t*BuNC under ambient conditions leads to the displacement of the ligand **L** which reacts with *t*BuNC to produce the known compound **14**[42] as shown in Scheme 2. The resulting iron complex, most likely $(CO)_4Fe(CNtBu)$[43] has not been isolated. On the other hand, carbon disulfide or acetone fail to displace the ligand **L** from the complex **1**.

The ^{11}B-NMR spectra of compounds **1 a–e** show only one signal around $\delta = 59$ which represents no significant change from the parent compound **1**. The ^{31}P-NMR spectra contain only one signal downfield from the resonance of the respective free phosphanes used. The coordination shifts, $\Delta^{31}P = \delta_{complex} - \delta_{free\ ligand}$, are consistent with the π-acidic character of the phosphanes. Since $P(OR)_3$ is a good π acceptor but not a good σ donor, the phosphorous atom would be expected to be more shielded in **1 d** than in the free ligand, and this is supported by its negative $\Delta^{31}P$ value.

In the IR spectra of **1 a–e**, three strong absorptions are found in the carbonyl region. Since PMe_3, Ph_2PMe, and $PhPMe_2$ are strong σ donors but weak π acceptors compared to PPh_3 or $P(OR)_3$, more effective π bonding to the remaining carbonyl in the equatorial position would be expected for **1 a–c** rather than in **1 d, e**. This expection is reflected in the positions of the CO streching frequencies. The band assigned to the equatorial CO group in **1 a–c** is observed between 1883 and 1886 cm^{-1} whereas the same band is found at 1964 and 1914 cm^{-1} for **1 d, e**, respectively.

In the ^{13}C-NMR spectra, recorded at room temperature, signals for carbonyl carbons appear as a broad singlet or as one doublet. However, the low-temperature limiting spectrum (at 210 K) of **1 a** consists of two doublets in a 1:2 ratio. The low intensity doublet found downfield is assigned to equatorial carbonyl carbons and the more intense one at higher field to equivalent axial carbonyl groups. As expected, the coupling constants $^2J(^{31}P^{13}C)$ observed in **1 a** are smaller than those of the $P(OMe)_3$ complex[16], implying a weaker Fe–P interaction in the former case. In order to compare the structural features of a phosphane-substituted complex with that of the parent complex **1**, the structure of **1 a** has been determined by X-ray crystallography.

Scheme 2

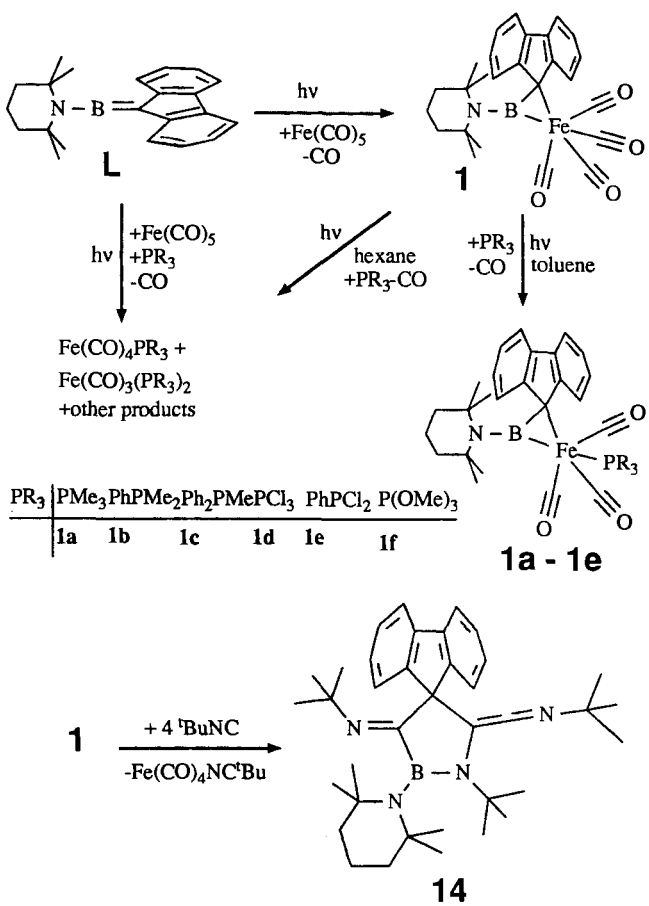

Molecular Structure of $Fe(CO)_3(\eta^2\text{-}tmpB=CR_2)(PMe_3)$ in the Solid State

The ORTEP plot of the molecule **1 a** is shown in Figure 10. As in complex **1**, the geometry around the iron atom is

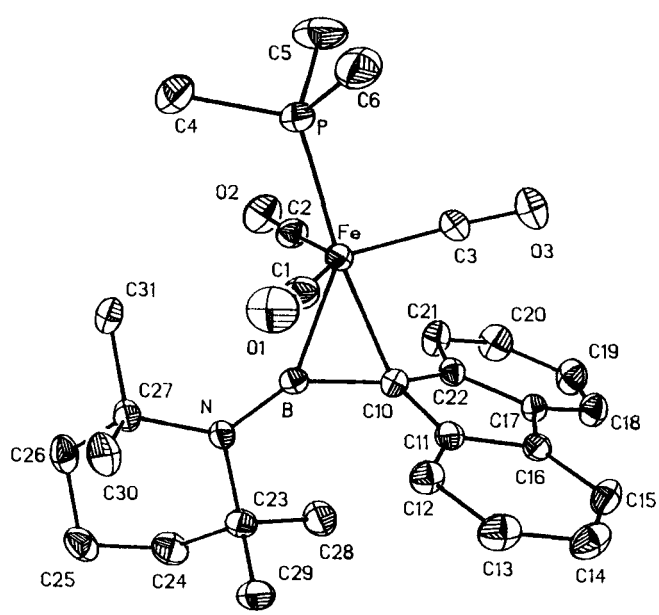

Figure 10. ORTEP plot of a molecule **1 a** in the crystal. Thermal ellipsoids are drawn on the 25% probability level

best described as distorted trigonal bipyramidal, the distortion being more pronounced in **1a** due to the steric requirement of the PMe_3 group in one of the axial positions. Its influence on the structure is clearly reflected by the bond angle C1 – Fe – C2, observed as 138.1(2)°. This is much smaller than the 151.2(2)° found in complex **1**. According to Hoffmann et al.[22a], the electronically preferred arrangement for complexes of the type $Fe(CO)_3(\eta^2$-olefin)D (D = strong σ donor) would be with D in an axial and the olefin in an equatorial position. Although this kind of arrangement has been proved by the structures of many complexes[44], a few exceptions do exist[45] where phosphanes occupy an electronically less favoured equatorial position. This is generally rationalized in terms of steric effects dominating the electronic site preference and, therefore, determining the final ligand arrangement. The binding of PMe_3 in the axial position can also be rationalized for the same reasons since the tmp – B = CR_2 ligand is too bulky as compared with diethyl fumarate[45b]. As expected, the equatorial Fe – C bond length, 1.785(4) Å, is shortened by 0.035 Å compared to the same bond in **1** [1.820(5) Å] while no appreciable change is observed in the axial bond length (shortened only by 0.01 Å). The Fe – P bond length 2.229(2) Å is slightly longer than the Fe – P bond length reported for $Fe(CO)_3(\eta^2$-tmp – B = $CR_2)[P(OMe)_3]$[16]. This corroborates with the coupling constant values $^2J(^{31}P^{13}C)$.

The B – C bond length in **1a** is slightly longer than in **1**. A perfect plane results from the group Fe,P,C3,X (X = midpoint of B = C), and the planes formed by the atoms Fe,P,C3,B and Fe,P,C3,C10 lie almost parallel to the Fe,P,C3,X plane as shown by the interplanar angles of 1.3 and 1.4°, respectively. The Fe – B and Fe – C10 bonds [2.091(4) and 2.159(4) Å, respectively] are shorter as compared to the corresponding bonds in **1** [2.125(5) and 2.190(4) Å, respectively] pointing to an increased (dp)π interaction. The C23 – N – C27 plane deviates significantly from the Fe – B – C10 plane with an interplanar angle of 18.3° (only 4.2° in **1**). The B – N bond length in **1a** [1.393(4) Å] is a little longer than in **1**, but still retains its double bond character.

This work has been supported by *Fonds der Chemischen Industrie*, *BASF Aktiengesellschaft*, and *Chemetall GmbH*. We are also grateful to Dipl.-Chem. *M. Thomann* for some final calculations, to Mrs. *D. Ewald* for recording many mass spectra, to Mrs. *G. Hanatschek* for measuring the IR spectra, and to Mr. *K. Schönauer* for performing the elemental analyses.

Experimental

All reactions were carried out in purified oxygen-free dry nitrogen gas by using standard Schlenk techiques. Toluene was purified by distillation from potassium or sodium benzophenone ketyl under nitrogen. Similarly, pentane and hexane were purified by distillation from $LiAlH_4$, and dichloromethane previously dried with calcium chloride, was finally destilled over P_4O_{10}. The ligand (9-fluorenylidene)(2,2,6,6-tetramethylpiperidino)borane (**L**)[10b,f], $Fe_2(CO)_9$[46] and $(C_6H_6)Cr(CO)_3$[47], $(PPh_3)_2Pt(C_2H_4)$[48] were prepared by literature procedures. $Cp'Mn(CO)_3$, $CpCo(CO)_2$, $Ni(COD)_2$, PPh_3, PPh_2Me, $PhPMe_2$, PCl_3, $PhPCl_2$, and PMe_3 (1 M solution in toluene) were used as received from commercial sources. $Fe(CO)_5$ was purified by trap-to-trap destillation before use.

NMR: Jeol FX 90Q (^1H), Bruker AC 200 (^{11}B, ^{13}C, and ^{31}P), Jeol FX 270 (^1H, ^{13}C) spectrometers. Standards: internal TMS (^1H), internal $CDCl_3$ (^1H, ^{13}C), internal CD_2Cl_2 (low-temperature ^{13}C-NMR spectra), internal C_6D_6 (^1H, ^{13}C), external $BF_3 \cdot OEt_2$ (^{11}B), external 85% aqueous H_3PO_4 (^{31}P). – IR: Varian FT 342, recorded in Nujol or in CCl_4. – MS: Atlas CH7, electron impact, 70 eV. – X-ray structure determinations: Syntex-Nicolet R3 diffractometer, SHELXTLS program, version 4.1, for structure solution and refinement. – Melting points: determined on analytically pure samples, sealed in evacuated or nitrogen-filled capillaries, uncorrected. – Elemental analyses; Microanalytical laboratory of the Institute.

Synthesis of the Complexes: All photochemical reactions were carried out in a quartz apparatus using a mercury lamp (Hanau Q 150) immersed in the solution of the reactands. Liberated CO gas was monitored volumetrically.

Tetracarbonyl[η^2-9-fluorenylidene(2,2,6,6-tetramethylpiperidino)borane]iron (**1**)[14] – *Improved Synthesis:* Irradiation of **L** (2.2 g, 7.0 mmol) and $Fe(CO)_5$ (1.0 ml, 7.1 mmol) in 70 ml of toluene for 1.5 h resulted in a dark brown solution which was filtered, concentrated to ≈ 10 ml and then layered with ≈ 20 ml of pentane. On cooling to −20°C for 4 d a dark brown crystalline product separated which was filtered, washed carefully with chilled pentane (2 × 5 ml) and thoroughly dried in vacuo. Yield: 2.1'g of **1** (64%), m.p. 136 – 140°C (dec.).

$C_{26}H_{26}BFeNO_4$ (483.2) Calcd. C 64.62 H 5.42 N 2.90
Found C 64.15 H 5.90 N 2.91

Carbonyl(η^5-cyclopentadienyl)[η^2-9-fluorenylidene(2,2,6,6-tetramethylpiperidino)borane]cobalt (**2**): **L** (2.21 g, 7.01 mmol) and $CpCo(CO)_2$ (2.0 g, 7.1 mmol) were irradiated in ≈ 70 ml of toluene for 12 h whereby 155 ml of CO gas evolved (uncorrected burette measurement). The apparatus was flushed with nitrogen before the lamp was turned off (it was found that, if the light was turned off and the solution allowed to stand under CO, the CO gas was taken up very rapidly by the solution). After filtration to separate small amounts of insoluble material all volatile components were removed from the filtrate in vacuo. The resulting nonvolatile red-brown oil was redissolved in ≈ 20 ml of toluene and the solution layered with ≈ 20 ml of hexane. Cooling the solution to −20°C for 12 h and to −70°C for another 2 h yielded a red-brown crystalline solid which was filtered, washed with pentane (2 × 5 ml), and dried in vacuo. An IR spectrum indicated the presence of a small amount of $CpCo(CO)_2$ besides **2**. Therefore, the solid was recrystallized from toluene/hexane (10:1; 25 ml), washed with cold pentane (2 × 5 ml), and dried in vacuo. Yield: 1.51 g of **2** (51%), m.p. 115°C (dec.). – NMR (C_6D_6)[19]: δ^1H: CH_3: 0.76, 2.09, 2.37 (3 s, intensity 1:2:1, 12 H), CH_2: 1.50 – 1.57, 1.72 – 1.82 (m, 6 H), $C_{13}H_8$: 7.19 – 7.23 (6 H, m), 7.80 – 7.86 (m, 2 H), Cp: 4.56 (5 H). – $\delta^{13}C$: 16.7 (C4), 31.5, 33.5, 34.2, 37.1 (C7/8), 39.1, 39.7 (C3/5), 56.8, 59.9 (C2/6), 89.2 (C of Cp), 21.7 (C9), 120.5, 120.7 (C14, C14′), 122.8, 123.1 (C11, C11′), 124.9, 126.3 (C12, C12′), 124.2, 124.4 (C13, C13′), 137.6, 138.0 (C15, C15′), 155.9, 157.4 (C10, C10′), 205.1 (CO). – IR (CCl_4): $\tilde{\nu}$ = 1958 cm^{-1} (νCO).

$C_{28}H_{31}BCoNO \cdot 1/2C_7H_8$ (513.4) Calcd. C 73.69 H 6.87 N 2.73
Found C 70.27 H 6.83 N 2.98

Dicarbonyl[η^2-9-fluorenylidene(2,2,6,6-tetramethylpiperidino)borane](η^5-methylcyclopentadienyl)manganese (**3**): Freshly distilled $Cp'Mn(CO)_3$ (1.40 g, 6.4 mmol) and **L** (2.00 g, 6.4 mmol) were irradiated in 70 ml of toluene for 12 h whereby ≈ 140 ml of CO

gas evolved (uncorrected burette measurement). The resulting dark-green solution was transferred into a 100-ml Schlenk flask, and all volatile components were removed in vacuo to leave a yellow-green oil which was dissolved in 10 ml of toluene. The solution was layered with 20 ml of hexane. From this mixture a yellow microcrystalline solid separated on cooling to −20°C for 12 h and to −78°C for another 3 h. The product was isolated, washed with pentane (2 × 5 ml), and dried in vacuo. Yield: 2.10 g of **3** (65%); m.p. 131−134°C. − NMR (C_6D_6)[19]: δ^1H: tmp and CH_3 of MeCp: 0.61, 1.66, 2.01 (m, braod, 21 H), Cp: 3.63, 3.90 (2 s, 4 H), aromatic protons: 7.10−7.23 (m, 6 H), 7.80−7.86 (m, 2 H). − δ^{11}B: 58.0. − δ^{13}C: 15.7 (C4), 32.9 (C7/8), 38.6, 39.5 (C3/5), 59.0, 63.3 (C2/6), 12.9 (CH_3Cp), 89.8, 90.9 (C_4H_4CMe), 101.9 (C_4H_4CMe), 119.8 (C14, C14′), 122.0 (C11, C11′), 124.5 (C12, C12′), 125.0 (C13, C13′), 136.3 (C15, C15′), 158.4 (C10, C10′), 24.2 (C9), 230.5 (CO). − IR (CCl_4): $\tilde{\nu}$ = 1937 and 1876 cm^{-1} (νCO).

$C_{30}H_{33}BMnNO_2$ (505.4) Calcd. C 71.30 H 6.58 N 2.77
Found C 71.09 H 6.85 N 2.68

(η^6-Benzene)dicarbonyl[η^2-9-fluorenylidene(2,2,6,6-tetramethylpiperidino)borane]chromium (**4**): The ligand **L** (2.38 g, 7.5 mmol) and $(C_6H_6)Cr(CO)_3$ (1.62 g, 7.5 mmol) were dissolved in 70 ml of toluene and irradiated for 12 h. 170 ml of CO gas was liberated. A light orange-coloured powder separated from the solution which was removed by filtration, washed with toluene (5 ml) and pentane (3 × 5 ml) and dried in vacuo. Yield: 2.60 g of **4**, m.p. 114°C. − NMR (C_6D_6)[19]: ^{1}H: CH_3: 0.75, 2.16 (s, 12 H), CH_2: 1.12−1.49 (m, 6 H), C_6H_6: 3.81, 3.99 (s, s, 6 H), fluorenylidene: 7.06−7.60 (6 H), 7.91−8.02 (2 H). − δ^{11}B: 57.2. − δ^{13}C: 15.8 (C4), 26.2 (broad, C9), 32.7, 33.2 (C7/8), 38.6, 39.7 (C3/5), 59.7, 63.3 (C2/6), 97.8, 100.0, 104.3 (C_6H_6), 120.3 (C14, C14′), 121.2 (C11, C11′), 124.3 (C12, C12′), 125.1 (C13, C13′), 135.1, 13.52 (C15, C15′), 162.9, 163.1 (C10, C10′), 187.6, 188.2 (CO).

$C_{30}H_{32}BCrNO_2$ (501.4) Calcd. C 71.87 H 6.43 N 2.79
Found C 71.46 H 6.57 N 2.74

Phosphane Complexes of **1**: The compounds **1 a**−**e** were obtained as follows: The phosphane ligand and $Fe(CO)_5$ were irradiated together in toluene until 2 mol equivalents of CO were liberated (measured by a gas burette). Then the stoichiometric amount of the appropriate phosphane was added to the solution. Stirring was continued until the reaction was complete as monitored by ^{31}P-NMR spectrometry. The complexes separated in analytically pure form from toluene/hexane or toluene/pentane mixtures.

Tricarbonyl[η^2-9-fluorenylidene(2,2,6,6,-tetramethylpiperidino)borane](trimethylphosphane)iron (**1 a**): Prepared from **L** (1.43 g, 4.5 mmol), $Fe(CO)_5$ (0.70 ml, 5.0 mmol), and PMe_3 (4.5 ml of a 1 M solution in toluene). Yield: 1.82 g of **1 a** (69%), orange-coloured crystals, m.p. 168−170°C (dec.). − NMR[19]: δ^1H ($CDCl_3$): tmp: 0.78, 1.98, 1.74−1.52 (m) (18 H); PMe_3: 1.52 (d, 9 H), $^2J(^{31}P^1H)$ = 9.7 Hz; fluorenylidine: 7.10−7.90 (8 H). − δ^{11}B (toluene): 58.7. − δ^{13}C (C_6D_6): 16.3 (C4), 32.1, 32.7 (7/8), 39.4, 39.8 (C3/5), 57.5, 60.2 (C2/6), 193.5 [d, $^1J(^{31}P^{13}C)$ = 32 Hz, PMe_3], 119.8 (C14), 121.9 (C11), 123.05 (C12), 124.8 (C13), 136.2 (C15), 156.2 (C10), 212.0 (CO); δ^{13}C (in CD_2Cl_2 at 210 K): 24.4 (C9), 214.6 [d, $^2J(^{31}P^{13}C)$ = 18.6 Hz, equator CO], 209.55 [d, $^2J(^{31}P^{13}C)$ = 35 Hz, axial CO]; δ^{31}P (toluene/$CDCl_3$) 33.3 (Δ^{31}P = +96). − IR (Nujol): 1999, 1925 and 1886 cm^{-1}, ν(CO).

$C_{28}H_{35}BFeNO_3P$ (531.2) Calcd. C 63.31 H 6.64 N 2.64
Found C 62.10 H 6.73 N 2.39

Tricarbonyl(dimethylphenylphosphane)[η^2-9-fluorenylidene(2,2,6,6-tetramethylpiperidino)borane]iron (**1 b**): Obtained from **L** (1.2 g, 3.8 mmol), $Fe(CO)_5$ (0.58, 4.1 mmol), and $PhPMe_2$ (0.54 ml, 3.8 mmol). Yield: 1.42 g of **1 b** (63%), yellow powder, m.p. 154°C (dec.). − NMR[19]: δ^1H ($CDCl_3$): tmp: 0.85 (s), 1.73 s, 1.26−1.53 (m) (18 H); PMe_2: 1.20 [d, $^2J(^{31}P_1H)$ = 9.4 Hz], fluorenylidene and Ph: 6.9−7.9 (m) (13 H). − δ^{11}B (toluene): 61.0. − δ^{31}P (toluene/$CDCl_3$): 37.0 (Δ^{31}P = +84). − IR (Nujol): $\tilde{\nu}$ = 1989, 1928, and 1883 cm^{-1}.

$C_{33}H_{37}BFeNO_3P$ (593.3) Calcd. C 66.81 H 6.29 N 2.36
Found C 66.00 H 6.28 N 2.25

Tricarbonyl[η^2-9-fluorenylidene(2,2,6,6-tetramethylpiperidino)borane](methyldiphenylphosphane)iron (**1 c**): Obtained from **L** (1.07 g, 3.4 mmol), $Fe(CO)_5$ (0.5 ml, 3.5 mmol), and Ph_2PMe (0.6 ml, 3.4 mmol). Yield: 1.9 g of **1 c** (63%), orange crystals, m.p. 178−180°C (dec.). − NMR[19]: δ^1H ($CDCl_3$): tmp: 0.71 (s), 1.46−1.63 (m, 18 H); Me_2P: 2.01 [d, 3 H, $^2J(^{31}P^1H)$ = 8.8 Hz], fluorenylidene and Ph: 7.23−7.88 (m, 18 H). − δ^{11}B (toluene): 58.2. − δ^{13}C ($CDCl_3$): 16.60 (C14), 61.48 (C2/6), 20.51 [d, $J(^{31}P^{13}C)$ = 33 Hz, PMe], 120.02 (C14), 123.2 (C11), 124.12 (C12), 125.72 (C13), 138.1 (C15), 156.64 (C10), 211.8 (CO). − δ^{31}P (toluene/$CDCl_3$): 56.5 (Δ^{31}P = 83). − IR (Nujol). $\tilde{\nu}$ = 1993, 1922 und 1884 cm^{-1} (νCO).

$C_{38}H_{39}BFeNO_3P$ (655.4) Calcd. C 69.64 H 6.00 N 2.14
Found C 70.61 H 6.13 N 1.75

Tricarbonyl[η^2-9-fluorenylidene(2,2,6,6-tetramethylpiperidino)borane](trichlorophosphane)iron (**1 d**): Obtained from **L** (1.00 g, 3.17 mmol), $Fe(CO)_5$ (0.50 ml, 3.57 mmol), and PCl_3 (0.32 ml, 3.18 mmol). Yield: 1.35 g of **1 d** (71%), orange crystalline product, m.p. ≈ 124°C. − NMR[19]: δ^1H ($CDCl_3$): tmp: 0.77 s, 1.87 s, 1.77−1.80 m (18 H); fluorenylidene: 7.09−7.78 (m, 8 H). − δ^{11}B (toluene): 59.4. − δ^{13}C ($CDCl_3$): 16.0 (C4), 33.0, 34.2 (C7/8), 38.2, 38.7 (C3/5), 58.1, 62.0 (C6/2), 120.7 (C14), 124.0 (C11), 124.9 (C12), 126.3 (C13), 139.2 (C15), 152.1 (C10), 207.9 [d, $^2J(^{31}P^{13}C)$ = 46 Hz, CO]. − δ^{31}P (toluene/$CDCl_3$): 189.9 (Δ^{31}P = −30). − IR (Nujol): $\tilde{\nu}$ = 2041, 1985, and 1964 cm^{-1}.

$C_{25}H_{26}BCl_3FeNO_3P$ (592.5) Calcd. C 50.68 H 4.42 N 2.36
Found C 52.03 H 4.61 N 2.20

Tricarbonyl(dichlorphenylphosphane)[η^2-9-fluorenylidene(2,2,6,6-tetramethylpiperidino)borane]iron (**1 e**): Obtained from **L** (1.3 g, 4.1 mmol), $Fe(CO)_5$ (0.60 ml, 4.3 mmol), and $PhPCl_2$ (0.56 ml, 4.1 mmol). Yield: 1.70 g of **1 e** (65%), orange-yellow powder, m.p. 155°C (dec.). − NMR[19]: δ^1H ($CDCl_3$): tmp: 0.80 s, 1.99 s, 1.19−1.54 m (18 H); fluorenylidene and Ph: 6.78−7.7 m (13 H). − δ^{11}B (toluene): 59.1. − δ^{13}C ($CDCl_3$): 15.9 (C4), 32.7, 33.7 (C7/8), 38.5, 38.9 (C3/5), 57.9, 67.4 (C2/6), 119.7 (C14), 123.8 (C11/C12), 125.8 (C13), 137.8 (C15), 153.1 (C10), 208.7 (CO). − δ^{31}P (toluene/$CDCl_3$): 199.5 (Δ^{31}P = 38.5). − IR (Nujol: $\tilde{\nu}$ = 2013, 1954, and 1914 cm^{-1} (νCO).

$C_{31}H_{31}BCl_2FeNO_3P$ (634.1) Calcd. C 58.72 H 4.93 N 2.21
Found C 59.80 H 5.05 N 2.20

1-tert-Butyl-4(tert-butylimino)-5-(tert-butyliminomethyl)-2-(2,2,6,6-tetramethylpiperidino)spiro[1,2-azaborolidin-4,9′-fluorene] (**14**): Complex **1** (1.16 g, 2.40 mmol) and *t*BuNC (1.01 ml, 9.60 mmol) were stirred together in ≈ 40 ml of toluene at room temp. overnight. During this period, the dark brown colour of the reaction mixture changed to light yellow (δ^{11}B: 36.2). The solvent was then removed to leave approximately 10 ml of solution. This solution was layered with 10 ml of hexane, and the mixture was then kept at −20°C overnight. The yellow crystalline product formed during this time was isolated by filtration, washed with pentane (2 × 5 ml) and dried in vacuo. Yield: 0.8 g of 14 (59%), m.p. 186°C (dec.). All spectral (NMR, IR, MS) data agreed with an authenic sample[42].

$C_{37}H_{53}BN_4$ (564.7) Calcd. C 78.70 H 9.46 N 9.92
Found C 75.92 H 9.33 N 9.40

Table 3. Atomic coordinates ($\times 10^4$) and equivalent isotropic thermal parameters ($\times 10^3$ Å^2) of carbonyl(cyclopentadienyl)[9-fluorenylidene(tetramethylpiperidino)borane]cobalt **2**. Equivalent isotropic U_{eq} defined as one third of the trace of the orthogonalized U_{ij} tensor

	x	y	z	U(eq)
Co(1)	1050(1)	3091(1)	1478(1)	49(1)
B	1723(7)	2065(4)	1761(4)	44(3)
C(1)	1120(6)	2628(3)	2436(3)	41(2)
C(2)	2074(6)	3093(3)	3180(3)	39(2)
C(3)	3508(7)	3305(4)	3312(3)	53(3)
C(4)	4188(7)	3713(4)	4070(4)	63(3)
C(5)	3458(8)	3922(4)	4699(4)	67(3)
C(6)	2042(8)	3701(4)	4577(3)	57(3)
C(7)	1341(7)	3275(3)	3815(3)	44(2)
C(8)	-97(7)	2951(3)	3523(3)	45(3)
C(9)	-1210(8)	2947(4)	3936(4)	64(3)
C(10)	-2468(9)	2577(5)	3520(5)	86(4)
C(11)	-2663(8)	2201(5)	2718(5)	92(4)
C(12)	-1549(8)	2192(4)	2299(4)	71(3)
C(13)	-249(7)	2570(4)	2709(4)	49(3)
N	2342(5)	1320(3)	1518(3)	48(2)
C(14)	3071(8)	1097(4)	807(4)	60(3)
C(15)	4280(9)	567(5)	942(5)	97(4)
C(16)	3836(10)	-250(5)	1115(5)	100(4)
C(17)	2826(16)	-71(6)	1631(8)	252(12)
C(18)	2248(8)	671(4)	1958(4)	56(3)
C(19)	2896(20)	972(6)	2734(5)	350(17)
C(20)	883(12)	432(9)	1982(11)	387(23)
C(21)	2069(9)	645(5)	65(4)	108(4)
C(22)	3729(9)	1884(5)	690(5)	104(5)
C(23)	627(9)	4033(4)	932(4)	71(3)
C(24)	1978(8)	3780(4)	839(4)	63(3)
C(25)	2783(8)	3949(4)	1587(4)	65(3)
C(26)	1913(9)	4313(4)	2146(4)	70(3)
C(27)	598(9)	4378(4)	1744(5)	77(4)
C(28)	-128(8)	2344(4)	829(4)	67(3)
O(28)	-897(6)	1840(3)	343(3)	97(3)
Co(2)	854(1)	2498(1)	-2294(1)	49(1)
B'	1453(7)	2007(4)	-3328(4)	43(3)
C(1')	991(6)	2868(3)	-3290(3)	43(2)
C(2')	-371(7)	3149(4)	-3609(3)	46(3)
C(3')	-1693(7)	2738(4)	-3886(3)	58(3)
C(4')	-2779(7)	3163(6)	-4174(4)	76(4)
C(5')	-2534(9)	3977(5)	-4197(4)	75(4)
C(6')	-1243(8)	4392(4)	-3940(4)	66(3)
C(7')	-136(7)	3985(4)	-3647(3)	48(3)
C(8')	1311(7)	4256(3)	-3374(3)	48(3)
C(9')	2057(9)	5022(4)	-3312(4)	67(3)
C(10')	3475(10)	5109(5)	-3074(4)	84(4)
C(11')	4166(8)	4454(5)	-2902(4)	77(4)
C(12')	3454(7)	3694(4)	-2952(4)	62(3)
C(13')	2005(7)	3598(4)	-3179(3)	45(2)
N'	2012(5)	1308(3)	-3804(3)	50(2)
C(14')	2687(8)	641(4)	-3471(4)	70(3)
C(15')	2756(12)	-179(5)	-4103(6)	136(6)
C(16')	3055(10)	-1£1(5)	-4855(6)	108(5)
C(17')	2108(9)	384(4)	-5176(4)	85(4)
C(18')	2192(7)	1295(4)	-4639(4)	58(3)
C(19')	3558(8)	1780(4)	-4634(5)	92(4)
C(20')	1003(7)	1724(4)	-4989(4)	71(3)
C(21')	1836(10)	396(5)	-2927(5)	129(6)
C(22')	4094(9)	997(5)	-3005(6)	138(6)
C(23')	605(14)	2631(9)	-1144(4)	104(5)
C(24')	498(11)	3410(8)	-1270(5)	97(5)
C(25')	1692(14)	3628(6)	-1457(4)	89(4)
C(26')	2597(9)	3037(9)	-1440(5)	98(5)
C(27')	1960(17)	2401(6)	-1241(5)	105(5)
C(28')	-535(8)	1756(4)	-2693(4)	61(3)
O(28')	-1473(6)	1251(3)	-2919(3)	90(3)
C(36)	3503(9)	7176(7)	470(8)	106(6)
C(33)	3321(13)	5994(9)	1198(10)	162(9)
C(32)	3395(13)	5758(8)	415(9)	151(8)
C(31)	3486(10)	6375(9)	71(8)	130(7)
C(35)	3442(10)	7426(7)	1261(9)	131(7)
C(34)	3334(9)	6842(8)	1645(7)	119(6)
C(37)	3567(11)	6125(8)	-752(7)	193(9)

X-ray Structure Determinations: Samples were mounted in sealed glass capillaries in an argon atmosphere. Graphite-monochromated Mo-K_α radiation was used. Cell parameters were determined from the setting angles of 20–25 high-angle centred reflections. Data collection was performed at 20°C by using ω scans with scan speeds varying from 2–29.3°/min according to count rates. 2 check reflections were monitored after every 48 intensity measurements. Lp and absorption correction (ψ scans) were applied. All structures were solved by direct methods. Calculations used full-matrix least-squares methods. Nonhydrogen atoms were described anisotropically. Hydrogen atoms were included in the final refinement with fixed U_i. As far as possible, refinement of the atomic coordinates for H were included as variables (**3**) or as a riding model (**1 a**, **2**). Definitions are: $R = \Sigma(|\Delta F|/\Sigma|F_o|)$, $R_w = [\Sigma w(\Delta|F|)^2/\Sigma w|F_o|^2]^{1/2}$, $w = [\sigma(F_o) + g(F_o^2)]^{-1}$. Atomic coordinates and equivalent isotropic temperature factors are summarized in Tables 3–5[49].

Table 4. Atomic coordinated (x 10^4) and equivalent isotropic thermal parameters (x 10^3 Å^2) of dicarbonyl[9-fluorenylidene(tetramethylpiperidino)borane](methylcyclopentadienyl)manganese **3**. U_{eq} see Table 3

	x	y	z	U
Mn	8666(1)	3705(1)	7056(1)	31(1)*
C(1)	6231(4)	3545(3)	7169(3)	27(1)*
C(2)	4912(4)	2978(3)	6205(3)	28(1)*
C(3)	4716(5)	3392(4)	5329(3)	35(1)*
C(4)	3325(5)	2700(4)	4526(3)	44(2)*
C(5)	2129(5)	1575(4)	4596(3)	45(2)*
C(6)	2275(5)	1163(4)	5465(3)	39(2)*
C(7)	3668(4)	1864(3)	6283(3)	31(1)*
C(8)	4133(4)	1684(3)	7285(3)	31(1)*
C(9)	3351(5)	752(4)	7750(3)	40(2)*
C(10)	4079(5)	832(4)	8730(3)	46(2)*
C(11)	5590(5)	1802(4)	9254(3)	40(2)*
C(12)	6387(5)	2739(4)	8807(3)	35(1)*
C(13)	5670(4)	2679(3)	7818(3)	29(1)*
B	7387(5)	4968(4)	7550(3)	28(1)*
N	7373(4)	6205(3)	7962(2)	30(1)*
C(14)	8933(5)	7441(4)	8462(3)	36(1)*
C(15)	8555(6)	8720(4)	8383(3)	48(2)*
C(16)	7110(6)	8818(4)	8736(4)	56(2)*
C(17)	5604(6)	7654(4)	8118(4)	51(2)*
C(18)	5729(5)	6292(4)	8138(3)	39(2)*
C(19)	10267(5)	7483(4)	7947(3)	46(2)*
C(20)	9618(6)	7448(4)	9558(3)	53(2)*
C(21)	5618(7)	5939(5)	9123(4)	58(2)*
C(22)	4209(5)	5333(4)	7317(4)	53(2)*
C(23)	8758(6)	1822(4)	7305(4)	51(2)*
C(24)	10299(5)	2580(4)	7201(4)	51(2)*
C(25)	9978(6)	2802(4)	6246(4)	50(2)*
C(26)	8253(5)	2185(4)	5741(3)	45(2)*
C(27)	7516(5)	1590(4)	6415(4)	48(2)*
C(28)	7441(8)	2091(6)	4681(4)	69(3)*
C(29)	8958(5)	4904(4)	6340(3)	40(2)*
O(1)	9183(4)	5578(3)	5792(3)	62(2)*
C(30)	9968(5)	4584(4)	9251(3)	41(2)*
O(2)	10939(4)	5041(3)	9034(2)	63(1)*

2: Single crystals grown from toluene solution, crystal size: 0.3 × 0.22 × 0.35 mm^3, a = 9.721(3), b = 16.560(5), c = 17.998(5) Å, α = 106.72(2), β = 98.58(2), γ = 91.95(3)°, V = 2735(2) Å^3, Z = 4; triclinic space group: $P\,1\,bar$ (No. 2), $F(000)$ = 1084, $\varrho_{calc.}$ = 1.247 g · cm^{-3}, μ = 6.50 cm^{-1}; 2Θ = 2–48° in h, +/−k, +/−l, max/min. transmission = 0.6413/0.5103, 9508 reflections measured, 7998 unique and 4948 considered observed [$I > 4\sigma(I)$], 640 variables, R = 0.059, R_w = 0.0578, g = 0.000379, Δ_{max}/σ = 0, ϱ_{max} = 0.48 e/Å^3. – The compound crystallized from toluene solution as a solvate with one molecule of toluene for the two independent molecules **2**. The termal parameters of the atoms C19, C20, and C17 as well as C22′, C21′, and C15′, respectively, indicate disorder in the

Table 5. Atomic coordinates (x 10^4) and equivalent isotropic thermal parameters (x 10^3 Å^2) of tricarbonyl[9-fluorenylidine(tetramethylpiperidino)borane](trimethylphosphane)iron **1a**. U_{eq} sec Table 3

	x	y	z	U(eq)
Fe	2534	779	6614	35(1)
C(1)	2475(4)	-434(3)	7532(3)	49(1)
O(1)	2390(4)	-1269(3)	8047(3)	79(1)
C(2)	3586(4)	1342(4)	5601(3)	47(1)
O(2)	4245(3)	1659(3)	4897(3)	71(1)
C(3)	986(3)	1494(3)	6563(3)	41(1)
O(3)	4(3)	1992(3)	6565(3)	63(1)
P	1810(1)	-463(1)	5293(1)	53(1)
C(4)	2837(5)	-1697(5)	4966(5)	80(2)
C(5)	1481(8)	160(7)	3911(4)	102(3)
C(6)	268(5)	-1140(6)	5612(5)	94(2)
C(10)	3015(3)	2071(3)	7878(3)	36(1)
C(11)	2282(3)	1962(3)	8927(3)	36(1)
C(12)	2258(4)	1069(3)	9708(3)	46(1)
C(13)	1501(4)	1210(5)	10657(3)	57(1)
C(14)	778(4)	2210(4)	10810(3)	58(1)
C(15)	807(4)	3098(4)	10038(4)	51(1)
C(16)	1570(3)	2995(3)	9101(3)	38(1)
C(17)	1873(3)	3825(3)	8225(3)	38(1)
C(18)	1517(4)	4980(3)	8091(4)	53(1)
C(19)	2023(5)	5610(4)	7221(4)	62(1)
C(20)	2863(5)	5078(4)	6495(4)	60(1)
C(21)	3224(4)	3927(4)	6610(3)	51(1)
C(22)	2741(3)	3282(3)	7498(3)	38(1)
B	4162(3)	1292(3)	7616(3)	34(1)
N	5460(3)	1089(2)	7960(2)	36(1)
C(23)	6111(4)	1907(4)	8849(3)	50(1)
C(24)	7594(4)	1975(5)	8710(4)	63(1)
C(25)	8267(3)	828(5)	8647(3)	60(1)
C(26)	7683(4)	197(4)	7655(4)	58(1)
C(27)	6185(3)	-24(3)	7687(3)	44(1)
C(28)	5603(5)	3151(4)	8702(5)	69(2)
C(29)	5814(4)	1495(5)	10032(3)	66(2)
C(30)	5911(4)	-949(4)	8554(4)	62(2)
C(31)	5772(5)	-472(4)	6523(4)	64(1)

tetramethylpiperidino groups. Calculations with a split model did not improve the result.

3: Single crystals grown from hexane solution, crystal size: 0.12 × 0.2 × 0.4 mm^3, yellow plates, a = 8.806(5), b = 10.905(3), c = 14.319(4) Å, α = 98.37(2), β = 103.77(3), γ = 107.05(3)°, V = 1241.9(8) Å^3, triclinic space group: $P1\,bar$ (No. 2), Z = 2, $F(000)$ = 532, d_{calc} = 1.351 g · cm^{-3}, μ = 5.37 cm^{-1}; 2Θ = 2–50° in h, +/−k, +/−l, 5057 reflections measured, 4726 unique and 3263 considered observed at the $I > 3\sigma(I)$ level, 406 variables, max/min. transmission = 0.939/0.883, 406 variables, R = 0.058, R_w = 0.062, g = 0.00183, ϱ_{max} = 0.33 e/Å^3.

1a: Single crystals form toluene/hexane, crystal size = 0.2 × 0.32 × 0.45 mm^3, a = 10.235(5), b = 11.525(7), c = 11.909(9) Å, β = 92.55(5)°, V = 1403.4(15) Å^3, monoclinic space group, $P2_1$ (No. 4), Z = 2, d_{calc} = 1.257 g · cm^{-3}, $F(000)$ = 560, μ = 6.2 cm^{-1}; 2Θ = 2–50° in h, +/−k, +/−l, 5463 reflections measured, 4913 unique and 4809 observed [$I > 3\sigma(I)$], max./min. transmission: 0.641/0.544, 337 parameters, R = 0.053, R_w = 0.054, g = 0.00113, ϱ_{max} = 0.75e/Å^3.

Appendix: The molecular-orbital calculations are of the Extended Hückel type[33] with atomic parameters for Fe[50] taken from earlier work; those for C, B, O, H are standard ones[33]. A modified Wolfsberg-Helmholz formula for calculating the H_{ij} matrix elements was used[51]. The model geometry for $(CO)_4Fe(H_2NBCH_2)$ employed the following interatomic distances and angles: Fe–CO = 180 pm; C–O = 114 pm; Fe–C_{H2} = Fe–B = 215 pm; C–B = 151.8 pm; B–N = 137.7 pm; N–H = 100 pm; C–H = 110 pm; C_{H2}–B–N_{H2} = 120°; H–C–H = 115° (hydrogen atoms on Fe–C–B bisector plane); C_c–Fe–C_d = 90°. Distortion angles optimized as detailed in the text.

CAS Registry Numbers

1: 116725-86-1 / **1a**: 136736-61-3 / **1b**: 136736-62-4 / **1c**: 136736-63-5 / **1d**: 136736-64-6 / **1e**: 136736-65-7 / **2**: 136736-57-7 / **2**·0.5 C_7H_8: 136736-58-8 / **3**: 136736-29-9 / **4**: 136736-60-2 / **6**: 136736-66-8 / **14**: 136708-38-8 / **L**: 96097-03-9

[1] Part 209: H. Nöth, J. Schübel, *Chem. Ber.* **1991**, *124*, 1963–1972.

[2] K. B. Gilbert, S. K. Boocock, S. G. Shore, *Comprehensive Organometallic Chemistry*, Chapter 41.1 and references therein (Eds.: G. Wilkinson, F. G. A. Stone, E. W. Abel), Pergamon Press, Oxford, **1982**.

[3] K. C. Kotz, D. G. Pedrotty, *J. Organomet. Chem.* **1970**, *22*, 425–438; H. Nöth, U. Schuchardt, *ibid.* **1970**, *22*, 435–440; J. M. Burlitch, M. J. Leonowicz, R. E. Hughes, *Inorg. Chem.* **1974**, *13*, 2203–2207; M. Fishwick, H. Nöth, W. Petz, M. G. H. Wallbridge, *ibid.* **1976**, *15*, 490–492.

[4] T. J. Marks, R. J. Kolb, *Chem. Rev.* **1977**, *77*, 263–293; B. G. Segal, S. J. Lippard, *Inorg. Chem.* **1978**, *17*, 844–850; J. C. Whitner, S. J. Cyvin, *J. Mol. Struct.* **1978**, *50*, 21–28; J. C. Whitner, B. N. Cyvin, S. J. Cyvin, *ibid.* **1979**, *53*, 281–286; R. J. Kinney, W. D. Jones, R. G. Bergmann, *J. Am. Chem. Soc.* **1978**, *100*, 7902–7915; R. T. Baker, D. W. Ovenall, R. L. Harlow, St. A. Westcott, N. J. Taylor, T. B. Marder, *Organometallics* **1990**, *9*, 3028–3030.

[5] G. Schmid, *Angew. Chem.* **1970**, *82*, 920–930; *Angew. Chem. Int. Ed. Engl.* **1970**, *9*, 819–828; G. Schmid, H. Nöth, *J. Organomet. Chem.* **1967**, *7*, 129–134; G. Schmid, H. Nöth, *Z. Anorg. Allg. Chem.* **1966**, *345*, 69–78; G. Schmid, H. Nöth, *J. Organomet. Chem.* **1966**, *5*, 109–119; G. Schmid, H. Nöth, *Angew. Chem.* **1963**, *75*, 861–862; G. Schmid, H. Nöth, *Chem. Ber.* **1968**, *101*, 1205–1214; C. S. Cundy, H. Nöth, *J. Organomet. Chem.* **1971**, *30*, 135–143.

[6] J. Knorr, J. S. Merola, *Organometallics* **1990**, *9*, 3008–3010; R. T. Baker, D. W. Ovenall, J. C. Calabrese, *J. Am. Chem. Soc.* **1990**, *112*, 9399–9400; Ch. Einertshofer, H.Nöth, M. Thomann, unpublished results (Ch. Einertshofer, Ph. D. Thesis, to be submitted).

[7] R. N. Grimes, *Comprehensive Organometallic Chemistry*, Chapter 5.5 and references therein (Eds.: G. Wilkinson, F. G. A. Stone, E. W. Abel); Pergamon Press, Oxford, **1982**.

[8] L. J. Todd, *Adv. Organomet. Chem.* **1970**, *8*, 87–115; W. Siebert, *ibid.* **1986**, *25*, 199–236.

[9] G. Huttner, W. Gartzke, *Chem. Ber.* **1974**, *107*, 3786–3789; W. Siebert, R. Full, H. Schmidt, J. von Seyerl, M. Halstenberg, G. Huttner, *J. Organomet. Chem.* **1980**, *191*, 15–25; W. Siebert, M. Bochmann, J. Edwin, C. Krüger, Y. H. Tsay, *Z. Naturforsch., Teil B*, **1978**, *33*, 1410–1416; J. A. K. Howard, I. W. Kerr, P. Woodward, *J. Chem. Soc., Dalton Trans.* **1975**, 2466–2469; P. S. Madden, A. Modinos, P. L. Timms, P. Woodward, *ibid.* **1975**, 1272–1277; G. E. Herberich, B. Hessner, S. Beswetherick, J. A. K. Howard, P. Woodward, *J. Organomet. Chem.* **1980**, *192*, 421–429.

[10] [10a] G. Maier, J. Henkelmann, H. P. Reisenauer, *Angew. Chem.* **1985**, *97*, 1061–1063; *Angew. Chem. Int. Ed. Engl.* **1985**, *24*, 1065–1067. – [10b] B. Glaser, H. Nöth, *Angew. Chem.* **1985**, *97*, 424–425; *Angew. Chem. Int. Ed. Engl.* **1985**, *24*, 416–417. – [10c] R. Boese, P. Paetzold, A. Tapper, *Chem. Ber.* **1987**, *120*, 1069–1071; R. Hunold, J. Allwohn, G. Baum, W. Massa, A. Berndt, *Angew. Chem.* **1988**, *100*, 961–963; *Angew. Chem. Int. Ed. Engl.* **1988**, *27*, 961–963. – [10d] H. Klusik, A. Berndt, *Angew. Chem.* **1983**, *95*, 895–896; *Angew. Chem. Int. Ed. Engl.* **1983**, *22*, 877–878. – [10e] A. Tapper, T. Schmitz, P. Paetzold, *Chem. Ber.* **1989**, *122*, 595–601. – [10f] B. Glaser, E. Hanecker, H. Nöth, H.-U. Wagner, *Chem. Ber.* **1987**, *120*, 659–667.

[11] [11a] P. Paetzold, *Adv. Inorg. Radiochem.* **1987**, *31*, 123–167, and references therein. – [11b] H. Nöth, *Angew. Chem.* **1988**, *100*, 1664–1684; *Angew. Chem. Int. Ed. Engl.* **1988**, *27*, 1603–1623, and references therein.

[12] [12a] K. Delpy, D. Schmitz, P. Paetzold, *Chem. Ber.* **1983**, *116*, 2994–2999. – [12b] P. Paetzold, K. Delpy, *Chem. Ber.* **1985**, *118*, 2552–2553. – [12c] H. Nöth, W. Rattay, U. Wietelmann, *Chem. Ber.* **1987**, *120*, 859–861. – [12d] H. Nöth, U. Wietelmann, *Chem. Ber.* **1987**, *120*, 863–865.

[13] [13a] B. Glaser, H. Nöth, *Chem. Ber.* **1986**, *119*, 3856–3858. – [13b] B. Glaser, Ph. D. Thesis, University of Munich, **1985**. – [13c] E. P. Mayer, Diploma Thesis, University of Munich, **1987**. – [13d] A. Tapper, Th. Schmitz, P. Paetzold, *Chem. Ber.*

1989, *122*, 595–601. – [13e] R. Boese, P. Paetzold, A. Tapper, R. Ziembinski, *Chem. Ber.* **1989**, *122*, 1057–1060.

[14] S. W. Helm, H. Nöth, *Angew. Chem.* **1988**, *100*, 1378–1384, *Angew. Chem. Int. Ed. Engl.* **1988**, *27*, 1331–1333.

[15] F. W. Grevels, D. Schultz, E. Koerner von Gustorf, *Angew. Chem.* **1974**, *86*, 558–560; *Angew. Chem. Int. Ed. Engl.* **1974**, *13*, 534–536.

[16] S. Channareddy, G. Linti, H. Nöth, *Angew. Chem.* **1990**, *102*, 222–224; *Angew. Chem. Int. Ed. Engl.* **1990**, *29*, 199–201.

[17] L. F. Kraus, Diplom Thesis, University of Munich, **1984**.

[18] ^{1}H and ^{13}C NMR data of Cp′Mn(CO)$_3$ are as follows: δ^1H: 1.48 (s, 3 H), 3.97 (s, 4 H); δ^{13}C: 13.2 (*Me*Cp), 82.3 (Me–*C*), 102.8 (MeCC_4), 225.6 (CO).

[19] For all ^{1}H- and ^{13}C-NMR spectral data the following numbering system for the tetramethylpiperidino group and the 9-fluorenyl ring is used:

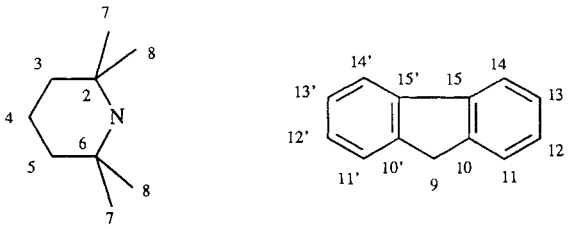

[20] The signal of the olefinic C atoms in (CO)$_4$Fe(C_2H_4) is found at δ^{13}C = 35.3, and the electronic structure of the molecule is discussed by W. E. Hill, C. H. Ward, T. D. Webbs, S. D. Worley, *Inorg. Chem.* **1979**, *18*, 2029–2030.

[21] F. A. Cotton, P. Lahnerta, *Inorg. Chem.* **1975**, *14*, 116–119.

[22] [22a] A. R. Rossi, R. Hoffmann, *Inorg. Chem.* **1975**, *14*, 365–374. – [22b] T. A. Albright, R. Hoffmann, I. C. Thibeault, D. L. Thorn, *J. Am. Chem. Soc.* **1979**, *101*, 3801–3812.

[23] J. Demuynck, A. Strich, A. Veillard, *Nouv. J. Chim.* **1977**, *1*, 217–229.

[24] M. Rossi, A. Sgamellotti, F. Tarantelli, C. Floriani, *Inorg. Chem.* **1987**, *26*, 3805–3811.

[25] M. I. Davis, C. S. Speed, *J. Organomet. Chem.* **1970**, *21*, 401–413.

[26] B. Beagley, D. G. Schmidling, D. W. J. Cruickshank, *Acta Crystallogr., Sect. B*, **1973**, *29*, 1499–1504.

[27] [27a] B. M. Chisnall, M. Green, R. P. Hughes, A. J. Wells, *J. Chem. Soc., Dalton Trans.* **1976**, 1899–1907. – [27b] T. H. Whitesides, R. W. Slaven, J. C. Calabrese, *Inorg. Chem.* **1974**, *13*, 1895–1899.

[28] C. J. Krüger, *J. Organomet. Chem.* **1970**, *22*, 697–706.

[29] L. R. Byers, L. F. Dahl, *Inorg. Chem.* **1980**, *19*, 277–284.

[30] A. F. Berndt, R. E. Marsen, *Acta Crystallogr.* **1963**, *16*, 118–123.

[31] B. Granoff, R. A. Jacobsen, *Inorg. Chem.* **1968**, *7*, 2328–2333.

[32] P. G. LeBorgne, E. Gentric, D. Grandjean, *Acta Crystallogr., Sect. B*, **1975**, *31*, 2824–2829.

[33] R. Hoffmann, *J. Chem. Phys.* **1963**, *39*, 1397–1412.

[34] Viewing **7** alternatively as derived from **8**, the (CO)$_d$ and (CO)$_c$ positions might imply to be of steric origin. Then the bending of the two axial CO's towards the boron atom remains to be explained.

[35] [35a] H. W. Spiess, R. Crosescu, W. Haeberlin, *Chem. Phys.* **1974**, *6*, 226–234. – [35b] L. Kruczynski, L. K. K. Li Shing Man, J. Takats, *J. Am. Chem. Soc.* **1974**, *96*, 4038–4040.

[36] E. Heilbronner, H. Bock, *Das HMO-Modell und seine Anwendung*, Verlag Chemie, Weinheim, **1968**; T. A. Albright, J. K. Burdett, M.-H. Wangbo, *Orbital Interactions in Chemistry*, J. Wyley and Sons, New York, **1985**.

[37] This deviation from an allene-type linear ligand geometry pushes up π-BC and lowers π*-BC below π*-BN. The latter is the LUMO if a linear allene-type $H_2N-B = CH_2$ structure is adopted.

[38] J. P. Collman, L. S. Hegedus, J. R. Norton, R. G. Finke, *Principles and Applications of Organotransition Metal Chemistry*, University Science Books, Mill Valley, Cal., **1987**.

[39] M. Elian, R. Hoffmann, *Inorg. Chem.* **1978**, *14*, 1058–1076; see also ref.[35b].

[40] It should be noted that the C_{3v}-to-C_s distortion of Fe(CO)$_4$ itself is unfavourable. Its energetic costs, however, are outweighed by the better bonding of L to the Fe(CO)$_4$ unit.

[41] The yellow product does not show an ^{11}B-NMR signal while the ^{31}P-NMR spectrum reveals two signals at δ = 82.9 and 74, indicating the presence of Fe(CO)$_4$(PPh$_3$) (R. L. Kreiter, E. A. Keiter, K. H. Hecker, C. A. Boecker, *Organometallics* **1988**, *7*, 2466–2469; J. J. Brunet, F. B. Kindela, D. Neibecker, *J. Organomet. Chem.* **1989**, *368*, 209–121) and Fe(CO)$_3$(PPh$_3$)$_2$. However, only the latter could be isolated in a pure form which shows δ^{31}P at 82.9; IR(Nujol): $\tilde{\nu}$ = 1876.1 cm^{-1} [ν(CO)]: $C_{39}H_{30}FeO_3$, Ber. C 70.5 H 4.55, Found C 70.85 H 4.7.

[42] E. P. Mayer, Ph. D. Thesis, University of Munich, **1989**.

[43] W. Hieber, D. v. Pigenot, *Chem. Ber.* **1956**, *89*, 193–201.

[44] J. S. Wood, *Progr. Inorg. Chem.* **1972**, *16*, 227–486.

[45] [45a] C. Krüger, Y. H. Tsay, *Cryst. Struct. Commun.* **1976**, *5*, 219–222. – [45b] M. V. R. Stainer, J. Takats, *Inorg. Chem.* **1982**, *21*, 4044–4049.

[46] E. H. Braye, W. Hübel, *Inorg. Synth.* **1966**, *7*, 178–180.

[47] E. O. Fischer, K. Öfele, *Chem. Ber.* **1957**, *90*, 2532–2535.

[48] U. Nagel, *Chem. Ber.* **1982**, *115*, 1998–1999.

[49] Further details on the crystal structure investigations are available on request from the Fachinformationszentrum Karlsruhe, Gesellschaft für wissenschaftlich-technische Information mbH, D-7514 Eggenstein-Leopoldshafen 2, on quoting the depository number CSD-55633, the names of the authors, and the journal citation.

[50] T. A. Albright, P. Hofmann, R. Hoffmann, *J. Am. Chem. Soc.* **1977**, *99*, 7546–7557.

[51] [51a] R. Hoffmann, P. Hofmann, *J. Am. Chem. Soc.* **1976**, *98*, 598–604. – [51b] J. H. Ammeter, H.-B. Bürgi, J. C. Thibeault, R. Hoffmann, *J. Am. Chem. Soc.* **1978**, *100*, 3686–3692.

[314/91]